CIAiS

Research and Education Consortium
for Innovation of Advanced Integrated Science

INTERNATIONAL SYMPOSIUM 2020

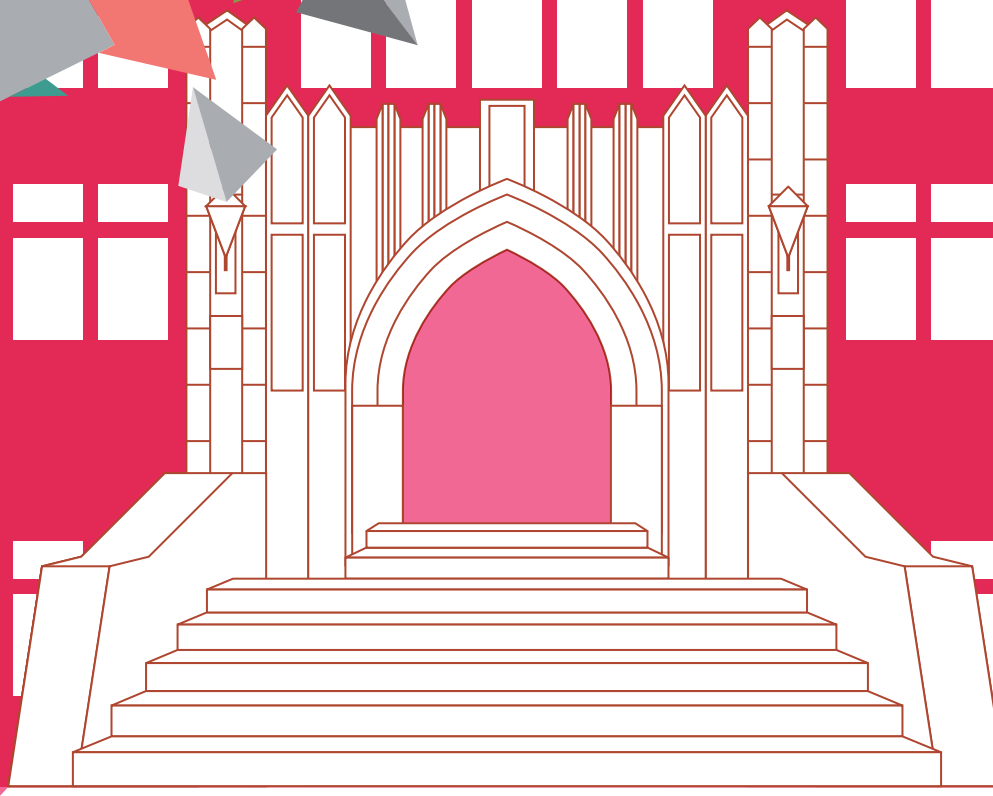

CIAiS
http://ciais.t.u-tokyo.ac.jp/

Friday, February28 13:30-19:00

**Room 213 1F Faculty of Engineering Bldg.2,
The University of Tokyo**

4 University Nano Micro Fabrication Consortium

THE UNIVERSITY OF TOKYO · Keio University · WASEDA University · Tokyo Institute of Technology · UEC TOKYO

Welcome Address

On behalf of the Research and Education Consortium for Innovation of Advanced Integrated Science (CIAiS), I would like to welcome all of you to the 2020 CIAiS International Symposium.

CIAiS is a cooperative effort between The University of Tokyo, Keio University, Waseda University, Tokyo Institute of Technology, and The University of Electro-Communications. Its partners are the National Institute for Materials Science (NIMS), RIKEN, and Kawasaki City. CIAiS began as a result of research produced by the Academic Consortium for Nano- and Micro-Fabrication, conducted through collaboration between the Four University Research Institute and the Advanced Photon Science Alliance (APSA). CIAiS brings together researchers from a wide range of fields to conduct new, high-quality, interdisciplinary research.

A stable, yet highly mobile employment system is used within the Consortium, in place of a more traditional short-term employment system where individuals are separated by institutions and departments. This is made possible as a result of budget provisions and an equalized system that transcends organizations. Next-generation researchers can engage in work while also considering career advancement. The Consortium provides post-docs and doctoral students with a variety of educational programs to facilitate experiences in different fields of study, help students develop a more comprehensive outlook, and to produce human resources who can work in diverse environments. We must encourage individuals who can innovate on a global scale. It is through these efforts that the Consortium aims to present researchers with career path models and increase the number of young people who would like to become researchers.

This symposium will give an overview of research efforts and will introduce the next-generation researchers at CIAiS. I hope the symposium will be a wonderful experience for all participants, and that it serves as an opportunity for new networks and research collaborations to begin.

Shigeo Maruyama
CIAiS Consortium Director
Professor, Department of Mechanical Engineering,
School of Engineering, The University of Tokyo

CIAiS International Symposium 2020

Table of Contents

CIAiS International Symposium 2020

Research and Education Consortium for Innovation of Advanced Integrated Science

Friday, February 28th, 2020 13:30-19:00

Room213, 1F, Faculty of Engineering Bldg. 2, The University of Tokyo

13:00 **Poster Open**

Opening 13:30-13:50

Chair: Yuta Yoshimoto

13:30-13:50 **Welcome Address**

Shigeo Maruyama

Consortium Director, The University of Tokyo

Opening Address

Keiji Yamamoto

Program Officer, Japan Science and Technology Agency

Keynotes 13:50-14:35

Chair: *Xiao-Mei Zhang, Tomotake Yamakoshi, Yasushi Shinohara*

13:50-14:05 **Coarse-grained molecular dynamics simulations on mechanical properties of polymer composites for bulk heterojunction solar cells**

Yuta Yoshimoto

Department of Mechanical Engineering, School of Engineering,

The University of Tokyo

14:05-14:20 **Clustering of phosphoinositides controls the binding modes of a membrane-bound protein on a biological membrane**

Eiji Yamamoto

Department of System Design Engineering, Keio University

14:20-14:35 **Toward a spectroscopic study of multi timescale, non-repeatable phenomena below one second**

Junko Omachi

Department of Chemistry, Kwansei Gakuin University

Next-generation Researchers 14:35-15:20

Chair:*, Xiao-Mei Zhang, Tomotake Yamakoshi, Yasushi Shinohara*

14:35 -14:50 **Coherent manipulation of ultracold Bosons in nonlinear Bloch bands**

Tomotake Yamakoshi

Institute for Laser Science, University of Electro-Communications

14:50-15:05 **p-type doped large-area multilayer MoS2 enabled by mild plasma treatment for UV phototransistors application**
Xiao-Mei Zhang
Department of Chemical Science and Engineering; Department of Mechanical Engineering, Tokyo Institute of Technology

15:05-15:20 **Theoretical study on high-order harmonic generation reflecting spatiotemporal symmetries**
Yasushi Shinohara
Photon Science Center, School of Engineering, The University of Tokyo

15:20-15:40 Break

Poster Presentation 15:40-16:15
Chair: Tomotake Yamakoshi, Yasushi Shinohara

15:40-16:15 Poster 1 min Presentation

Poster Session 16:15-17:15
Chair: Xiao-Mei Zhang

16:15-17:15 Poster Session

Closing 17:15-17:30
Chair: *Yuta Yoshimoto*

17:15-17:30 **Closing Remarks**
Hitoki Yoneda
Institute for Laser Science, University of Electro-Communications

Social Gathering 17:30-19:00
Chair: *Tomotake Yamakoshi, Yasushi Shinohara*

17:30-19:00 Social Gathering
CIAiS Poster Awards

Keynotes

Coarse-grained molecular dynamics simulations on mechanical properties of polymer composites for bulk heterojunction solar cells

Yuta Yoshimoto

Department of Mechanical Engineering, The University of Tokyo

yyoshimoto@fel.t.u-tokyo.ac.jp

Organic solar cells (OSCs) possess light-weight, flexible, and stretchable features along with the diversity of molecular designs compared to the inorganic counterparts, although they have historically suffered from low power conversion efficiencies (PCEs). As such, a great number of studies have mainly focused on improving PCEs, resulting in the OSC with a PCE of about 17% [1]. In contrast, much less work has been devoted to improve mechanical properties of OSCs, which is also key to OSC-installed flexible and wearable devices.

In the present study, we investigate mechanical properties of polymer composites of regioregular poly(3-hexylthiophene) (P3HT) and fullerene C_{60} using coarse-grained molecular dynamics (CGMD) simulations, where the P3HT monomer unit and C_{60} are represented by three CG beads and a single CG bead [2,3], as depicted in Fig. 1(a). The tensile simulations illustrated in Fig. 1(b) indicate that pure P3HTs with the degrees of polymerization (DPs) of 50, 100, and 150 exhibit almost identical tensile moduli, while the tensile strength increases with the DP. We quantify an increase in the number of molecular chain entanglements [4] resulting from

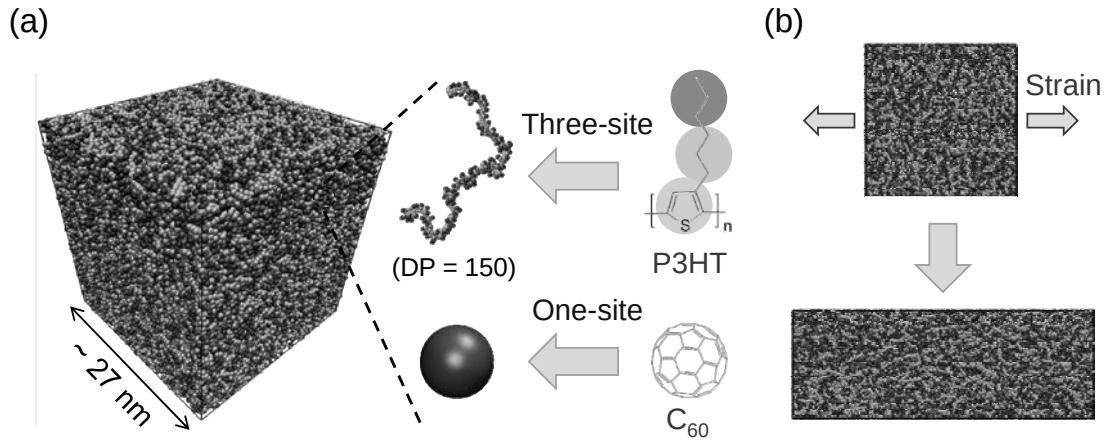

FIG. 1. (a) A representative CGMD system of a P3HT:C_{60} composite with a degree of polymerization (DP) of 150 and a C_{60} mass fraction of 50%. (b) Uniaxial tensile simulations are performed with a strain rate of 10^{-4} ps^{-1}.

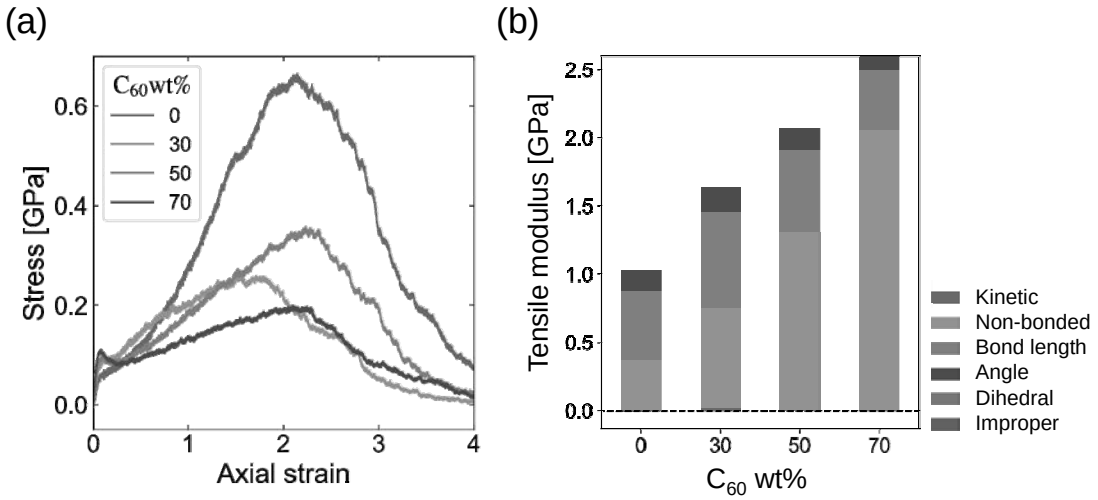

FIG. 2. (a) Stress–strain curves for the C_{60} mass fractions of 0, 30, 50, and 70% (DP = 150). Tensile moduli are calculated from the slopes of the curves in the linear elastic regions. (b) Contributions to the tensile moduli from kinetic energy, non-bonded interaction, and bonded-interactions composed of bond length, angle, dihedral, and improper potentials.

increasing DP, which in turn enhances the tensile strength. Meanwhile, the decomposition of molecular interactions contributing to stress indicates that the tensile modulus is primarily determined by non-bonded potentials and bond length potentials, almost independent of the chain entanglements. Furthermore, as shown in Fig. 2(a), the addition of C_{60} leads to higher tensile modulus and hence more brittle behavior of the composite in accordance with experiments [5]. We find that an increase in C_{60} mass fraction further inhibits molecular chain entanglements, leading to a significant reduction of the tensile strength. Meanwhile, an increase in the tensile modulus mainly originates from an increase in non-bonded interactions associated with C_{60}, as shown in Fig. 2(b).

Acknowledgements

This work was partly supported by Research and Education Consortium for Innovation of Advanced Integrated Science (CIAiS).

References

[1] Y. Lin et al., Adv. Mater. **31**, 1902965 (2019).

[2] K. N. Schwarz et al., Nanoscale **5**, 2017 (2013).

[3] S. E. Root et al., Macromolecules **49**, 2886 (2016).

[4] M. Kröger, Comput. Phys. Commun. **168**, 209 (2005).

[5] S. Savagatrup et al., Adv. Funct. Mater. **24**, 1169 (2014).

Clustering of phosphoinositides controls the binding modes of a membrane-bound protein on a biological membrane

Eiji Yamamoto
Department of System Design Engineering, Keio University
eiji.yamamoto@sd.keio.ac.jp

Membrane-bound domains within peripheral membrane proteins have a function to localize the proteins on biological membrane surfaces. The pleckstrin homology (PH) domain is a binding module possessed by a wide range of peripheral membrane proteins, which interacts with phosphatidylinositol phosphates (PIPs) in membranes. Multi-scale molecular dynamics simulation study provides insights into the molecular details of interaction and dynamics of PH domains on biological membranes [1-3]. Here, we will show the effect of local PIP enrichment on the interaction of PH domains with membranes [4]. The binding energy of a PH domain to PIP_3-containing lipid membranes increases according to the increase of PIP_3 concentration. The binding free energy of the PH domain with more than two PIP_3 molecules is of the same order as experimental values. The PH domain exhibits three different binding modes on the membrane surface depending on the local concentration of PIP_3. These results suggest that local nanoscale clustering of PIP molecules in a membrane can control the strength and orientation of the PH domain interaction.

References

[1] E. Yamamoto, A.C. Kalli, T. Akimoto, K. Yasuoka, and M.S.P. Sansom, "Anomalous Dynamics of a Lipid Recognition Protein on a Membrane Surface", *Sci. Rep.* **5**, 18245 (2015).
[2] E. Yamamoto, A.C. Kalli, K. Yasuoka, and M.S.P. Sansom, "Interactions of Pleckstrin Homology Domains with Membranes: Adding Back the Bilayer via High Throughput Molecular Dynamics", *Structure* **24**, 1421 (2016).
[3] E. Yamamoto, T. Akimoto, A.C. Kalli, K. Yasuoka, and M.S.P. Sansom, "Dynamic Interactions between a Membrane Binding Protein and Lipids Induce Fluctuating Diffusivity", *Science Adv.* **3**, e1601871 (2017).
[4] E. Yamamoto, J. Domański, F.B. Naughton, R.B. Best, A.C. Kalli, P.J. Stansfeld, and M.S.P. Sansom, "Multiple Lipid Binding Sites Determine the Affinity of PH Domains for Phosphoinositide-Containing Membranes", *Science Adv.* **6**, eaay5736 (2020).

Toward a spectroscopic study of multi-timescale, non-repeatable phenomena below one second

Junko Omachi
Department of Chemistry, Kwansei Gakuin University
junko.omachi@kwansei.ac.jp

Our goal is to make a spectroscopic tool to enable to investigate an initial process of non-repeatable phenomena. The dynamics across multi timescale below one second is of particular interest to us. For example, protein dynamics range from electron transfer and vibrational motions at femto- and pico-second timescales and to conformational change at millisecond or even longer timescales. There are several experimental methods to observe these dynamics, including time-resolved X-ray scattering, nuclear magnetic resonance spectroscopy, and laser-based spectroscopy. These methods have their limitations and applicable timescales. Among them, we believe that laser-based measurements have potential to capture successive dynamics from the ultrafast timescale. Although their spatial resolution is the order of the wavelength of light, which is larger than the size of targets, they offer electronic and structural information of materials spectroscopically. For example, pump-probe spectroscopy is commonly used to study ultrafast electronic dynamics on femtosecond-picosecond timescales. Also, time-resolved spectroscopies with a Streak camera enable us to take successive temporal dynamics on their limited time ranges. However, in principle both optical techniques cannot take temporal dynamics on multi timescale successively. So, we are planning to make a new spectroscopic method to capture data on multi-timescale. There are many difficulties. One of them is how we take multi-timescale data of one event and how we deal with massive data. It is not smart to take data from femtosecond to one second by fixed time-step. In this presentation, I will talk about our on-going project.

Next-generation Researchers

Coherent manipulation of ultracold Bosons in nonlinear Bloch bands

Tomotake Yamakoshi
Institute for Laser Science, University of Electro-Communications
t_yamakoshi@ils.uec.ac.jp

Ultracold atoms and molecules have been eagerly investigated since the experimental realization of Bose-Einstein condensates and quantum degenerate Fermi gases. Their high controllability and visibility render the systems suitable for the investigation of atomic interferometers, quantum simulators, and so forth. Especially, the ultracold atomic system with optical lattices has attracted much attention since the systems are ideal for simulating various Hamiltonian systems. In recent years, unconventional phenomena in higher bands have attracted much attention to developing new quantum technologies.

One of the intriguing topics is coherent wave packet preparation of a target state with high fidelity. Especially, coherent population transfer onto a specific band is a prerequisite for achieving coherent quantum control over a wide range of phase space in the optical lattice system. Recently, an experimental group in Beijing demonstrated that the “standing-wave pulse sequence” method could produce the wave packet in higher bands very efficiently[1]. It repeatedly turns the optical lattice on and off and applies time-wise pulses of the impulse to confined ultracold atoms with appropriate time intervals. Recently, we developed a theoretical extension of their experimental works with ideal(non-interacting limit) ultracold Bosonic atoms. We numerically explored optimal pulse-sequence parameters and found an optimized sequence which excites more than 99% of the atoms to first and second excited bands without atom-atom interaction[2]. However, the atom-atom interaction is non-negligible, causing the dephasing of the wave packet. In the treatment of ultracold Bosonic systems, the interaction is often represented by a nonlinear term in the framework of the mean-field approximation. In addition to the dephasing, the strong nonlinear term modulates the band structure and Bloch waves, thus altering the wave packet dynamics in the optical lattice[3].

In this talk, we present the numerical results of coherent population transfer by the standing-wave pulse sequence method with a one-dimensional bichromatic optical lattice system for the major purpose of producing dense and robust wave packets. We demonstrate that the excited wave packet is very robust with appropriate parameters due to an unconventional

parabolic dispersion of the bichromatic lattice. In addition, we examine a nonlinear effect due to the atom-atom interaction. We numerically found that the standing-pulse sequence method works well in the nonlinear system. We show that the process can produce robust wave packet which consists of nonlinear Bloch waves. The coherent manipulations of ultracold Bosons with optical lattice and nonlinearity may pave the way for investigating low-dimensional quantum properties subject to a designed band structure.

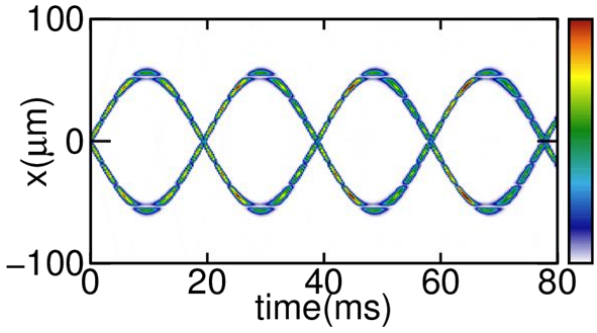

Fig1. Time evolution of stable wave packet in the combined potential of the bichromatic lattice and the harmonic potential.

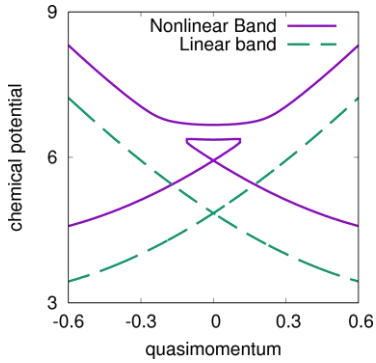

Fig2. 1st and 2nd excited dispersion of linear Bloch(dashed) band and nonlinear Bloch band(solid).

References

[1] X. Zhou, S. Jin, and J. Schmiedmayer, New J. Phys. 20, 055005(2018).

[2] Tomotake Yamakoshi and Shinichi Watanabe, Phys. Rev. A 99, 013621(2019).

[3] Dmitri Diakonov, L. M. Jensen, C. J. Pethick, and H. Smith, Phys. Rev. A 66, 013604 (2002)

p-Type Doped Large-Area Multilayer MoS_2 Enabled by Mild Plasma Treatment for UV Phototransistors Application

Xiao-Mei Zhang

Department of Mechanical Engineering, School of Engineering, Tokyo Institute of Technology

zhang.x.as@m.titech.ac.jp

Two-dimensional (2D) transition metal dichalcogenides (TMDCs), such as MoS_2, have attracted considerable attention owing to the unique optical and electronic properties related to its 2D ultrathin atomic layer structure. MoS_2 is becoming prevalent in post-silicon digital electronics and in highly efficient optoelectronics due to its extremely low thickness and its tunable band gap (E_g = 1–2 eV) [1]. In order to develop 2D MoS_2 photodetectors with ultrafast response and high responsivity, up-scalable techniques for realizing controlled *p*-type doping in MoS_2 is necessary. For low-power, high-performance complementary logic applications, both *p*- and *n*-type MoS_2 FETs (NFETs and PFETs) must be developed. The fabrication of MoS_2 FETs with complementary *p*-type characteristics is challenging due to the significant difficulty of injecting holes into its inversion channel. One approach is to use unconventional contacts resulting in a low Schottky barrier height for hole injection in MoS_2 PFETs. For example, MoOx ($2 < x < 3$) contacts have been shown to be effective for hole injection into pristine MoS_2 [2]. A proper interface between MoOx and MoS_2 layers is necessary for efficient hole injection. Examples initiated doping by incorporating substitutional niobium, Nb, atoms during chemical vapor deposition (CVD) growth and chemical doping with AuCl3 [3]. However, substitutional doping during CVD growth is lacking in area selectivity and the adoption of $AuCl_3$ would be hampered by the risk of Au contamination.

In this work, we demonstrate a *p*-type multilayer MoS_2 photodetector with selective-area doping using CHF_3 plasma treatment, as shown in Fig.1a. The grown MoS_2 nanosheets were subjected to out-of-plane doping by CHF_3 plasma treatment using a dry-etching system (ULVAC original NLD-570). The radiofrequency power of this dry-etching system was set to 100 W and the pressure was set to 7.5 mTorr. The final thickness of the treated samples was obtained by etching for 30 s. Fig. 1b shows the optical micrograph (OM) image of the selective-area MoS_2 films with and without CHF_3 plasma treatment. XPS analysis was carried out to investigate the binding energies of Mo and F in the CHF_3-treated and untreated MoS_2 samples. Fig. 1c shows the detailed binding energy profiles of Mo for the CHF_3-treated and untreated MoS_2 samples,

respectively. In comparison, all relevant peaks of the CHF_3-treated sample were broader and red-shifted. This red-shift of peaks indicates the proper *p*-type doping of MoS_2 nanosheets. The specific types of dopants introduced by the plasma processes were confirmed by the XPS spectra in Fig.1d. A prominent binding energy peak associated with F was observed in CHF_3-treated samples, while the F peak was absent for untreated samples. Back-gated *p*-type MoS_2 FETs are fabricated with an on/off current ratio in the order of 10^3 and a field-effect mobility of 65.2 $cm^2V^{-1}s^{-1}$. They exhibit gate-modulated UV photodetection with a rapid response time of 37 ms. This study provides a promising approach for the development of mild plasma-doped MoS_2 as a 2D material in post-silicon electronic and optoelectronic device applications.

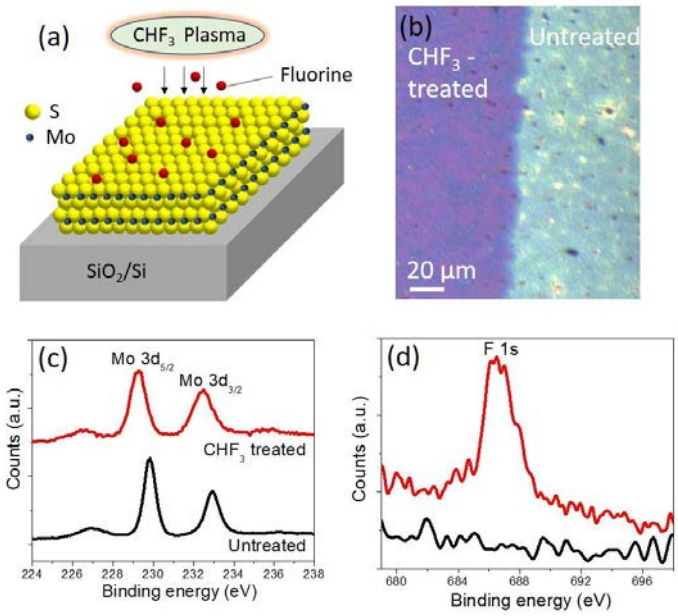

Figure 1. (a) Schematic diagram of MoS_2 nanosheets subjected to out-of-plane doping by CHF_3 plasma treatment. (b) OM image of the selective-area MoS_2 films with and without CHF_3 plasma treatment. (c) XPS spectra for Mo signals before and after plasma treatment. (d) XPS spectra for MoS_2 exhibit the presence of the F 1s peak in CHF_3 plasma-treated MoS_2.

References:

1. Jeong, S.H.; Liu, N.; Park, H.; Hong, Y.K.; Kim, S. Temperature-dependent electrical properties of Al_2O_3 passivated multilayer MoS_2 thin-film transistors. Appl. Sci. 2018, *8*, 424.
2. Chuang, S.; Battaglia, C.; Azcatl, A.; McDonnell, S.; Kang, J.S.; Yin, X.; Tosun, M.; Kapadia, R.; Fang, H.; Wallace, R.M. MoS_2 p-type transistors and diodes enabled by high work function MoOx contacts. Nano Lett. 2014, *14*, 1337.
3. Das, S.; Demarteau, M.; Roelofs, A. Nb-doped single crystalline MoS_2 field effect transistor. Appl. Phys. Lett. 2015, *106*, 173506.

Theoretical study on high-order harmonic generation reflecting spatiotemporal symmetries

Yasushi Shinohara
School of Engineering, The University of Tokyo
shinohara@atto.t.u-tokyo.ac.jp

A frontier of optical science is extreme nonlinear optical responses of crystalline solids under intense coherent light with much smaller photon energy than the typical bandgap of insulators [1]. The strength of the optical electric field is V/nm level invoking a typical field strength the valence electron feels in materials. The strong external perturbation shakes the system significantly, leading to strong nonlinear response beyond the perturbative regime.

The breakdown of the perturbation theory appears in a scaling law of high-order harmonic generation, photon energy upconversion. The intensity of second-order (third-order) harmonics is proportional to square (cubic) of the intensity of the driving field when the perturbation theory works. By increasing the driving field intensity, the harmonic intensities do not follow the order of harmonics [2]. A key question here is which physical signature in the nonperturbative regime is the same as a perturbative regime and not the same. This question is raised in a case that photon polarization emitted by high-order harmonic generation (HHG) from crystalline solids [3]. For the perturbative regime, the emitted photon polarization under an applied field direction is well understood by the nonlinear susceptibility tensors. The spatial symmetry of the target crystal restricts the component in the tensors, leading to selection rules. However, the selection rules rely on the perturbation theory. We showed that unexpected behavior appears in the HHG spectra [3] by experiments and theoretical simulations in the nonperturbative regime. We need a more general theory to explain the unexpected results beyond the perturbative expansion.

We propose a theory to describe HHG angle dependence to answer the question partially. We introduce a time-dependent polarization under a linearly polarized electric field with a specific angle between the crystal orientation. We apply a symmetry operation for the system, both material and the electric field simultaneously, in which the system is invariant under the operations. Then, we apply the same operation only for the electric field. In the two cases, the response, induced polarization, should be the same. This fact leads to an equation to restrict the component of the induced polarization. We apply the procedure to all allowed symmetries for

GaSe crystalline solid as an example. To derive the exact condition for the HHG, we introduce a new concept that *odd* and *even periodic function* for the polarization. The odd (even) periodic function shows (not) sign change with respect to half period shift, temporal symmetry. Combining these two symmetries, spatial and temporal, we derive an angle dependence of HHG for GaSe. The dependence perfectly reproduces the experimental result and the simulation.

[1] Stanislav Yu. Kruchinin, Ferenc Krausz, and Vladislav S. Yakovlev, Rev. Mod. Phys. **90**, 021002 (2018).

[2] S. Ghimire, A.D. DiChiara, E. Sistrunk, P. Agostini, L.F. DiMauro, and D.A. Reis, Nat. Phys.**7**, 138 (2011).

[3] K. Kaneshima, Y. Shinohara, K. Takeuchi, N. Ishii, K. Imasaka, T. Kaji, S. Ashihara, K. L. Ishikawa, and J. Itatani, Phys. Rev. Lett. **120**, 243903 (2018).

Poster Session

Poster Session

Poster No,	Name	Institution	Affiliation	Presentation Title
1	Hao-Sheng Lin	The University of Tokyo	Department of Mechanical Engineering	Highly Selective and Scalable Fullerene-Cation-Mediated Synthesis accessing Cyclo[60]fullerenes with 5-Membered-Carbon-Ring and their Application to Perovskite Solar Cells
2	Mizuki Tani	The University of Tokyo	Department of Nuclear Engineering and Management	Inter-atomic distance effects on high-harmonic generation from one-dimensional crystal
3	Toshihiro Kaneko	The University of Tokyo	Department of Mechanical Engineering	Relation between oxygen gas diffusivity and porous characteristics under capillary condensation of water in cathode catalyst layers of polymer electrolyte membrane fuel cells
4	Yutaro Isono	The University of Tokyo	Department of Nuclear Engineering and Management	Numerical implementation of time-dependent Hartree-Fock method on a curvilinear coordinate
5	Jongbeom Choi	Tokyo Institute of Technology	Department of Mechanical Engineering	Deposition of Ni - CNT composite film from Ni plated CNT by cold spray
6	Takuma Teramura	The University of Tokyo	Department of Nuclear Engineering and Management	Gauge-Invariant TDCIS Method for Molecular High-Field Science
7	Dongig OH	The University of Tokyo	Department fo Mechanical Engineering	Margination of Platelet-size Spherical Particles in Blood flow through the Branch of Microchannels
8	Kakeru Sasaki	The University of Tokyo	Department of Nuclear Engineering and Management	First-Principles Calculation of Nonlinear Optical Absorption upon Irradiation with a Two-Color Laser
9	Chihiro Kamijima	The University of Tokyo	Department fo Mechanical Engineering	Analysis of the Flow Mechanism in Micro Pulsating Heat Pipes Using Image Recognition
10	Seungchul OH	The University of Tokyo	Department of Mechanical Engineering	Modeling and Fabrication of Thermally-Actuated Bimetal Device
11	Hiroki Emura	The University of Tokyo	Department of Physics	Measurement of optical absorption in periodically poled MgO-doped SLT crystals with 532 nm CW laser
12	Hiroki Imai	The University of Tokyo	Department fo Mechanical Engineering	Analysis of non-equilibrium rarefied gas flows using low variance deviational simulation Monte Carlo
13	Takao Saiki	The University of Tokyo	Department of Precision Engineering	Development of ultrafast imaging system using the slicing mirror for understanding the mechanism of laser machining
14	Nana Takahashi	Waseda University	Department of Electronic and Physical Systems	Electrical property change of woody carbon material by moisture absorption
15	Yurina Michine	University of Electro-Communications	Institute for Laser Science	Ozone mixed gas grating for high power laser applications
16	Anna Suzuki	University of Electro-Communications	Institute for Laser Science	High Quality-factor Kerr-lens mode-locked Tm:Sc2O3 laser with SRS-based spectral broadening
17	Bokusui Nakayama	Keio University	Faculty of Science and Technology	Light Interference Assisted Widening the Wavelength Range of Gold Nanoparticles Coloring and Its Dynamic Control
18	Ryo Soma	Keio University	Graduate School of Science and Technology	Tunable Dynamics of Janus Particles by Coating Phase-change Material
19	Katsuyuki Enomoto	Keio University	Graduate School of Science and Technology	Optical observation of DNA translocation dynamics in SiN nanopore
20	Yutaka Ikeda	Tokyo Institute of Technology	Department fo Mechanical Engineering	The Development of Flow-type Thermo-electrochemical Conversion Combined with Forced Convection Cooling
21	Aoi Fuchi	University of Electro-Communications	Institute for Laser Science	Development of laser system of charge exchange process in J-PARC
22	Takahito Igawa	Chiba Institute of Technology	Graduate school of Engineering	Experiments on Polishing Epoxy Resin Surface of CFRP Mirror for Space Telescopes

Highly Selective and Scalable Fullerene-Cation-Mediated Synthesis accessing Cyclo[60]fullerenes with 5-Membered-Carbon-Ring and their Application to Perovskite Solar Cells

Hao-Sheng Lin

Department of Mechanical Engineering, The University of Tokyo

linhaosheng@photon.t.u-tokyo.ac.jp

In thin-film photovoltaics, cyclo[60]fullerenes have been widely used as electron acceptors in organic solar cells and as electron-transporting layers (ETLs) in perovskite solar cells. In particular, cyclo[60]fullerenes as an over-coating layer of metal oxide ETLs have been one of the most exploited applications in perovskite solar cells, demonstrating a dramatic reduction hysteresis and enhancement of the device charge-dynamics. With respect to such applications, heterocyclo[60]fullerene, which is one of the most abundant types of cyclo[60]fullerene, have shown relatively poor performance compared with full-carbon-ring cyclo[60]fullerenes because of their electrochemical instability. Accordingly, cyclo[60]fullerenes with a full-carbon-ring, such as 3-membered-carbon-rings (e.g. $PC_{61}BM$) and 6-membered-carbon-rings (e.g. ICBA, MIF), have been the preferred choices for the over-coating layers of metal oxide ETLs. However, cyclo[60]fullerenes with a 5-membered-carbon-ring, namely indano[60]fullerenes, have never been demonstrated to date because of inefficient synthetic protocols.

In this work, a fullerene-cation-mediated synthesis, accessing a new class of 5-membered-carbon-ring cyclo[60]fullerenes with high yields of up to 93% is showcased. This method utilizes aryl[60]fullerene cations, ArC_{60}^{+} as intermediates, which are generated in situ by heating the aryl[60]fullerenyl dimers in the presence of $CuBr_2$. In addition, 5-membered-carbon-ring cyclo[60]fullerenes display excellent device applicability when they are used in perovskite solar cells as over-coating layers of electron-transporting layers. A power conversion efficiency of 20.7% is achieved thanks to the favorable energy alignment, optimized substrate design, and electrochemical stability of the 5-membered-carbon-ring fullerenes.[1]

1. H.-S. Lin, I. Jeon, Y. Chen, X.-Y. Yang, T. Nakagawa, S. Maruyama, S. Manzhos, Y. Matsuo, *Chem. Mater* **2019**, *31*, 8432.

Inter-atomic distance effects on high-harmonic generation from one-dimensional crystal

[1]Mizuki Tani, [1,2]Yasushi Shinohara, [1,2,3]Takeshi Sato, [1,2,3]Kenichi L. Ishikawa

1: Department of Nuclear Engineering and Management, Graduate School of Engineering, The University of Tokyo

2: Photon Science Center, Graduate School of Engineering, The University of Tokyo

3: Research Institute for Photon Science and Laser Technology, The University of Tokyo

mzktani@atto.t.u-tokyo.ac.jp

Spectral features of high-order harmonic generation (HHG) are quite different between the solid and the gas phases. While HHG in the gas phase is well understood by the three-step model [1], investigating a comprehensive mechanism of solid-state HHG is still under active research field [2-4]. In order to bridge the gap between the solid-state and gas-phase HHG, we focus on inter-atomic distance (IAD) of periodic crystal, which is one of the parameters that smoothly connects atoms and solids. We investigate how the high-harmonic spectra change from solid-like to gas-like ones with increasing IAD.

We simulate HHG from one-dimensional model periodic systems by solving the time-dependent Schrödinger equation within the independent electron approximation. We use a local potential which has the ground-state level (= -14 eV) comparable to that of the hydrogen atom. The IAD is a distance between the periodically arranged potentials wells. The value is varied between 0.5 nm - 50 nm. We evaluate the HHG spectrum as a power spectrum of the current density. We consider a driving laser pulse with 1.55 eV (corresponds to 800 nm) central photon energy, 9 fs FWHM pulse duration, and 5.3×10^{13} W/cm^2 peak intensity. We identify two characteristic IAD regions by insights of spectral changes. Our analysis show that, while one is originated by a static effect due to a change of electronic structure, the other is due to a dynamic effect related with the electronic motion in the laser field.

[1] P. B. Corkum, Phys. Rev. Lett. 71 (1993) 1994.

[2] K. Kaneshima, Y. Shinohara, K. Takeuchi, N. Ishii, K. Imasaka, T. Kaji, S. Ashihara, K. L. Ishikawa, and J. Itatani, Phys Rev. Lett. 120 (2018) 243903.

[3] T. Ikemachi, Y. Shinohara, T. Sato, J. Yumoto, M. Kuwata-Gonokami, and K. L. Ishikawa, Phys. Rev. A 95 (2017) 043416.

[4] T. Ikemachi, Y. Shinohara, T. Sato, J. Yumoto, M. Kuwata-Gonokami, and K. L. Ishikawa, Phys. Rev. A 98 (2018) 023415.

Relation between oxygen gas diffusivity and porous characteristics under capillary condensation of water in cathode catalyst layers of polymer electrolyte membrane fuel cells

Toshihiro Kaneko[1*], Yuta Yoshimoto[1], Takuma Hori[2], Shu Takagi[1], Ikuya Kinefuchi[1]

[1] Department of Mechanical Engineering, The University of Tokyo

[2] Department of Mechanical System Engineering, Tokyo University of Agriculture and Technology

*Email: tkaneko@fel.t.u-tokyo.ac.jp (presenting author)

In the mesoporous cathode catalyst layer of polymer electrolyte membrane fuel cells, water arises as the electrical power generation process goes on through $O_2 + 4H^+ + 4e^- \rightarrow 2H_2O$. It is known that the generated water fills the catalyst layer through capillary condensation that results in a reduction of power generation performance due to a significant increase in the oxygen diffusion resistance, but little is known about the quantitative relation among the oxygen diffusion resistance, the mesoporous characters and the amount of condensed water. An effective porosity and tortuosity factor are important parameters to characterize porous structures. In the case of the cathode catalyst layer, the effective porosity changes through capillary condensation of water and this effect must be considered appropriately. Our group developed coupled analysis simulation of lattice density functional theory and gas transport simulation of Knudsen flow region and applied to the porous media composed of randomly packed spheres [1]. In this work, we applied this approach for the actual structure of the mesoporous cathode catalyst layer obtained by a focused ion beam scanning electron microscope [2]. First, the mesoporous cathode catalyst layer surrounded by bulk region is expressed as voxel data and the capillary condensation process of water is simulated by lattice density functional theory. Second, the oxygen diffusivity and the porous characters are calculated and the tortuosity factor is obtained. The calculated tortuosity factor, which is relevant to the oxygen diffusion resistance, is summarized as a function of effective porosity and they are compared to the Bruggeman equation.

References

[1] Y. Yoshimoto, T. Hori, I. Kinefuchi, and S. Takagi, *Phys. Rev. E* **96**, 043112 (2017).

[2] T. Kaneko, Y. Yoshimoto, T. Hori, S. Takagi, J. Ooyama, T. Terao, and I. Kinefuchi, *Int. J. Heat Mass Transf.*, **150**, 119277 (2020).

Numerical implementation of time-dependent Hartree-Fock method on a curvilinear coordinate

Yutaro Isono[1], Yasushi Shinohara[1], Takeshi Sato[1,2], Kenichi. L. Ishikawa[1,2]
[1]Graduate School of Engineering, The University of Tokyo
[2]Research Institute for Photon Science and Laser Technology, The University of Tokyo
Author e-mail address: y.isono@atto.t.u-tokyo.ac.jp

High-order harmonic generation (HHG) used to generate attosecond pulses is actively studied as one of the most important high-field phenomena [1]. The electron dynamics in such high-field phenomena are, in principle, exactly described by the time-dependent Schrödinger equation (TDSE); however, the computational cost of TDSE increases exponentially with respect to the number of electrons. In addition, the real-space simulation of high-field phenomena requires (i) a high spatial resolution in the vicinity of nuclei to accurately represent the electron-nucleus interaction and (ii) a good absorbing boundary to prevent unphysical reflection of photoelectrons at the edge of the simulation box. We have developed the time-dependent multiconfiguration self-consistent-field (TD-MCSCF) methods [2,3], that can efficiently describe intense laser-driven multielectron dynamics, and implemented these methods for atoms [4, 5] and molecules [6]. In this work, to investigate larger molecules, we implement the time-dependent Hartree-Fock method on a curvilinear coordinate, which satisfies the above-mentioned requirements (i) and (ii) simultaneously. We report the first application of the implementation to the HHG from molecules, such as C_2H_2 (ethylene).

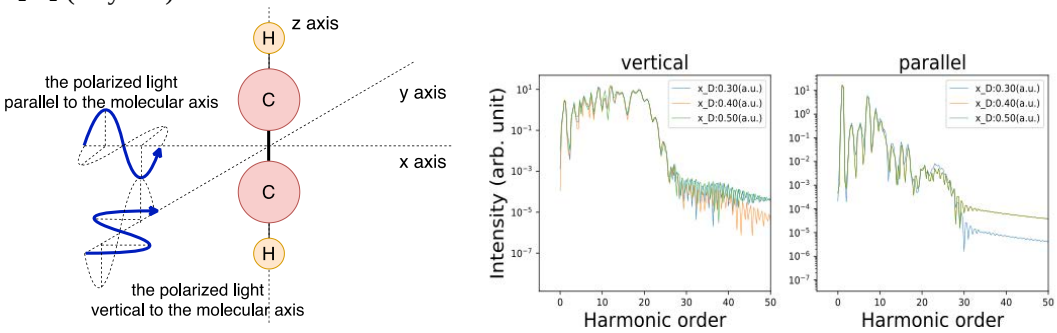

(a) (b) (c)

Fig. 1. HHG spectra from a C_2H_2 molecule exposed to a linearly polarized laser pulse with a wavelength of 800 nm, an intensity of 10^{14} W/cm^2, and a foot-to-foot duration of three optical cycles. (a) Relative orientation of the laser polarization and the molecule. (b) HHG spectra for the laser polarization perpendicular to the molecular axis. (c) HHG spectra for a laser polarization parallel to the molecular axis. Results with a fine (grid side lengths $\geq D = 0.3$ in atomic unit), medium ($D = 0.4$), and coarse ($D = 0.5$) grid discretization.

[1] H. W. van der Hart, Science 328, 1645 (2010).
[2] T. Sato and K. L. Ishikawa, Phys. Rev. A 88, 023402 (2013).
[3] T. Sato and K. L. Ishikawa, Phys. Rev. A 91, 023417 (2015).
[4] T. Sato, K. L. Ishikawa, I. Březinová, et al, Phys. Rev. A 94, 023405 (2016).
[5] Y. Orimo, T. Sato, A. Scrinzi, and K. L. Ishikawa, Phys. Rev. A 97, 023423 (2018).
[6] R. Sawada, T. Sato and K. L. Ishikawa, Phys. Rev. A 93, 023434 (2016).

Deposition of Ni - CNT composite film from Ni plated CNT by cold spray

Choi Jongbeom, Wataru Nakayama, Nana Okimura, Takuya Hotchi, Yuki Hirata, Naoto Ohtake, Hiroki Akasaka
Department of Mechanical Engineering, Tokyo Institute of Technology
E-mail: choi.j.ah@m.titech.ac.jp

Deposition of CNT metal matrix composites (CNT-MMC) films by thermal spray have attracted many attentions for enhancing characteristics of a film [1]. Cold spray technique, one of spray technique, is unique spray method that has lower temperature working gas than traditional spray techniques. Particles introduce into the low temperature working gas, and are accelerated up to supersonic speed. Accelerated particles collides with substrate and plastically deform. As a result, particle is possible to be deposited with less oxidation by the low temperature working gas. Due to this advantage, several studies on deposition of CNT-MMC were conducted [1]. On the other hand, CNT is too brittle, and is hard to obtain enough energy at collision to plastically deform because of its light weight. Therefore, CNT needs to be linked to another heavy weight material for applying of CS. Although the ball milling method fabricates uniformly distributed CNT-MMC by interlocking CNT on the surface, CNTs in the films suffer structural defect during the ball milling process [2].

In this study, we propose that chemically nickel coated CNT particle was prepared, and applied for the deposition of the high-density CNT-MMC. CNTs was coated with Ni by the electroless Ni plating method, and fabricated Ni coated CNT was applied to the CS technique.

Electroless Ni plating solution was prepared by mixing 30 g/L of Ni^{2+} solution (SEK-797-0; Kanigen Co., Ltd.) and 30 g/L of reductant solution (SEK-797-2; Kanigen Co., Ltd.). The plating solution was heated up to 85 °C, and stirred by magnetic bar. CNT (Baytube C70P; Bayer Materialscience) was dip into the solution for 30 mins to coat Ni. The composite films were deposited by a low-pressure cold spray technique (ACGS; Startack Co., Ltd.). Nitrogen in 600 °C and 0.6 MPa was used as acceleration gas. On CS deposition, spray nozzle was scanned 10 times over the Al substrate which was sand-blasted by #46 alumina.

Figure1 (a) shows the SEM image of Ni coated CNT particles. Ni particles with below 1 μm in diameter was grown in globular shape on the agglomerated CNT and each Ni particle was independent from others. Figure 1 (b) shows the surface SEM image of the deposited Ni coated CNT film. The agglomerated CNT was detected on the surface same as particles. This image indicated that agglomerated CNT which was linked with the grown Ni particles were deposited by deformation of metal components. Because the relatively heavy Ni with CNT particles were accelerated and obtained enough energy to be plastically deformed. GD-OES profile in Fig. 2 indicates that weight percent of carbon in the film was quite high and more than 50 wt.%.

These results indicated that Ni coated CNT with high-density was obtained by electroless Ni plating method and possible to be deposited with cold spray technique.

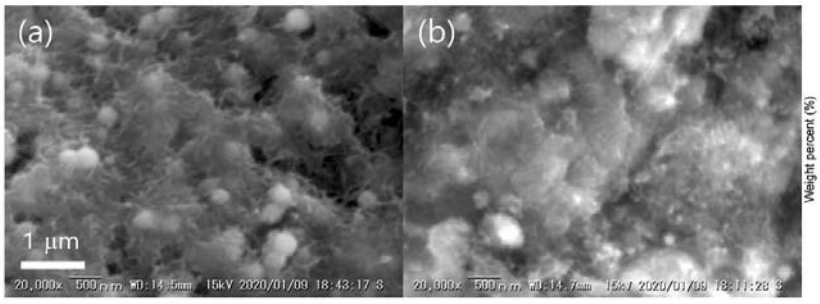

Figure 1. SEM images of Ni coated CNT particles (a) and film (b)

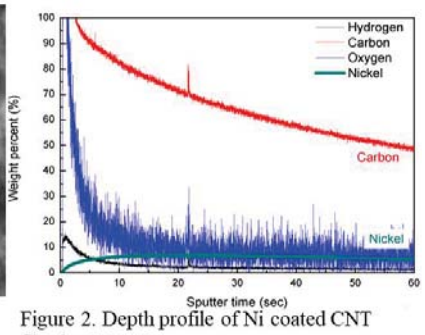

Figure 2. Depth profile of Ni coated CNT film by GDOES.

[1] T. Laha, et. al. Acta Materialia 55(2007) 1059, [2] S. Cho, et al., Surf. & Coat. Tech. 206 (2012) 3488.

Gauge-Invariant TDCIS Method for Molecular High-Field Science

Takuma Teramura, Takeshi Sato, and Kenichi L. Ishikawa
Department of Nuclear Engineering and Management,
Graduate School of Engineering, The University of Tokyo
teramura@atto.t.u-tokyo.ac.jp

High-harmonic generation (HHG) is highly nonperturbative electron dynamics triggered by intense laser fields. Recently, HHG in molecules has been investigated as a novel tool to explore molecular electronic structure. For theoretical investigation of high-field phenomena, various first-principles methods e.g. the time-dependent configuration interaction singles (TDCIS) method have been developed.

The TDCIS method models the system dynamics in terms of a linear combination of single excitation/ionization from the ground state. In the formulation by Rohringer *et al*. [1], the TDCIS wavefunction is written as

$$\Psi(r_1 \cdots r_N; t) = C_0(t)\Phi_{\mathrm{GS}}(r_1 \cdots r_N) + \sum_i \Phi_{\phi_i}^{\chi_i(t)}(r_1 \cdots r_N; t),$$

where Φ_{GS} is the Hartree-Fock ground state and $\Phi_{\phi_i}^{\chi_i(t)}$ is the singly-excited configuration replacing an orbital ϕ_i in the ground state with $\chi_i(t)$, an electronic wave packet originating from ϕ_i. The original formulation of the TDCIS method suffers from a violation of the gauge principle, namely, consistency between the length gauge and the velocity gauge of laser-matter interaction Hamiltonian. Although the velocity gauge has an advantage in terms of computational cost, the velocity gauge of the existing formulation gives wrong results.

To solve this dilemma, we have proposed the gauge-invariant reformulation of the TDCIS method which allows us to enjoy the numerical advantage of the velocity gauge [2,3]. In this contribution, we present the gauge-invariant reformulation and application to HHG from propane molecule.

[1] N. Rohringer, A. Gordon, and R. Santra, Phys. Rev. A **74**, 043420 (2006).
[2] T. Sato, T. Teramura, and K. L. Ishikawa, Appl. Sci. **8**, 433 (2018).
[3] T. Teramura, T. Sato, and K. L. Ishikawa, Phys. Rev. A **100**, 043402 (2019).

Margination of Platelet-size Spherical Particles in Blood flow through the Branch of Microchannels

Dongig Oh[*1], Satoshi Ii[*2], Shu Takagi[*1]

[*1] University of Tokyo, [*2] Tokyo Metropolitan University

dongig.oh@fel.t.u-tokyo.ac.jp

Platelets comprise an essential component of human blood due to their role in the coagulation process[1)]. These phenomena require that the platelets move close to the vessel wall, initiating platelet-wall contact followed by adhesion. It has been known that the red blood cells (RBCs) play a crucial role in platelets margination by expelling them toward the RBC-depleted zone near the vessels wall, resulting in near-wall excess (NWE)[2)].

In current study, Immersed Boundary Methods are used to simulate fluid-structure interface problem. we first investigated margination of platelet-size spherical particle in a square microchannel with different Capillary number (Ca) and Hematocrit (0,5,10,20,40) and compared the results with experimental data. The results showed good agreement with experimental data[3)]. From the results, we also estimated the diffusion coefficient of the particles in the margination process.

Finally, we conducted simulation with the branch of microchannels. We analyzed the reconstruction of NWE process in daughter channels and reports how the movement of RBCs effects the regeneration of NWE.

References

1. Wootton, D. M., and D. N. Ku. 1999, Fluid mechanics of vascular systems, disease, and thrombosis. *Annu. Rev. Biomed. Eng.* (1) 299-329
2. Eckstein, E. C. *et al.*, 1987, Transport of platelets in flowing blood. *Ann. N. Y. Acad. Sci.* (516) 442-452
3. Noso R., *et al.*, 2015, Cross-Sectional Distributions of Platelet-Sized Particles in Blood Flow through Microchannels. *Nihon Reoroji Gakkaishi.* (43) 99-104

First-Principles Calculation of Nonlinear Optical Absorption upon Irradiation with a Two-Color Laser

Kakeru Sasaki, Yasushi Shinohara and Kenichi L. Ishikawa

School of Engineering, The University of Tokyo

kakeru051113579@atto.t.u-tokyo.ac.jp

Nonlinear optical absorption is one of the most fundamental processes in high-intensity laser interaction with matter. In insulators with a wide bandgap, anisotropy does not appear in linear absorption but in nonlinear optical absorption [1]. Optimizing nonlinear absorption and clarifying the mechanisms behind it will lead to an understanding of the earliest stages of laser processing. It is reported that in the gas phase, the ionization rate can be controlled through the relative phase of a two-color laser [2]. In this study, first-principles calculations are used to investigate how nonlinear absorption in solids changes with the mixing ratio of two-colors. In this study, we use the SALMON code [3] to numerically solve the time-dependent Kohn-Sham equation and evaluate the absorption energy by calculating the difference between the energy after the laser pulse irradiation and the initial energy.

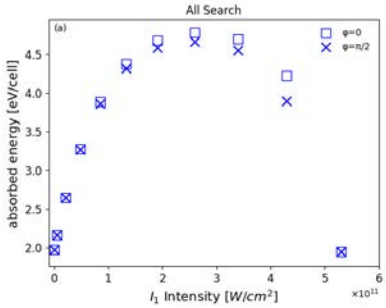

Fig. 1. (a) The nonlinear optical absorption as a function of 1.6eV laser intensity. Box and x marker represent nonlinear optical absorption for $\varphi = 0$ and $\pi/2$ respectively, where φ is a relative phase

Figure 1 shows the change in nonlinear absorption when the relative intensity between the 1.60 eV or 3.20 eV components is changed while fixing the sum at 5.308×10^{11} W/cm^2. It is found that the absorption energy is higher with two-color mixed laser fields than in the single-color cases. On the other hand, the results are insensitive to the relative phase between the two colors.

[1] M. Gertsvolf, et al, Phys. Rev. Lett. **101** (2008), 243001

[2] H. G. Muller, P. H. Bucksbaum, D. W. Schumacher and A Zavriyev, J. Phys. B: At. Mol. Opt. Phys. **23** (1990), 2761

[3] M. Noda, S. A. Sato, et al , Comp. Phys. Comm. **235** (2018) 356.

Analysis of the Flow Mechanism in Micro Pulsating Heat Pipes Using Image Recognition

Chihiro Kamijima[a], Yuta Yoshimoto[a], Shu Takagi[a], Ikuya Kinefuchi[a]

[a] Department of Mechanical Engineering, The University of Tokyo, 7-3-1 Hongo, Bunkyo-ku, Tokyo 113-8656, Japan

kamijima@fel.t.u-tokyo.ac.jp

Pulsating heat pipes (PHPs), which transfer heats via self-oscillation of liquid slugs, are considered as promising next-generation cooling devices thanks to their simple wickless structure and ease of miniaturization. However, complex flow mechanisms of PHPs have yet to be understood sufficiently, and optimal design guides to enhance thermal performances have not been fully revealed. In this study, we fabricate a micro-PHP with a hydraulic diameter of 350 μm, and measure the thermal conductivities using FC-72 as a working fluid. The micro-PHP tends to exhibit higher thermal conductivities for the filling ratio around 50% and the cooling temperature of 40 ˚C. We also record inner flows with a high speed camera and extract flow patterns using semantic segmentation, a deep learning based image recognition technique. An example of extracted flow pattern is illustrated in Fig. 1. It is revealed that liquid films on the channel walls become longer and thinner for higher thermal conductivity conditions, resulting in enhanced latent heat transfer. Additionally, we model inner flows and heat transfer of the micro-PHP, and conduct numerical analyses by substituting the extracted flow patterns into the model. As shown in Fig. 2, we find that latent heat transfer due to evaporation and condensation of liquid films accounts for a significant portion of the overall heat transfer, while sensible heat transfer by the liquid slugs is negligible small.

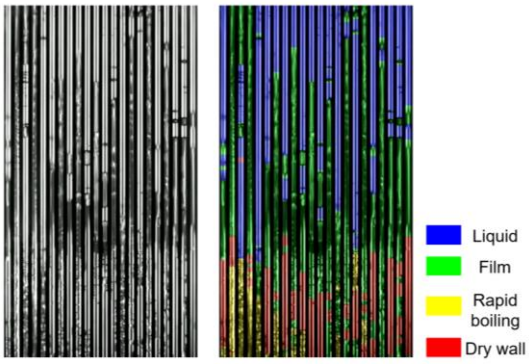

Fig. 1 Inner flows and corresponding flow patterns extracted by image recognition

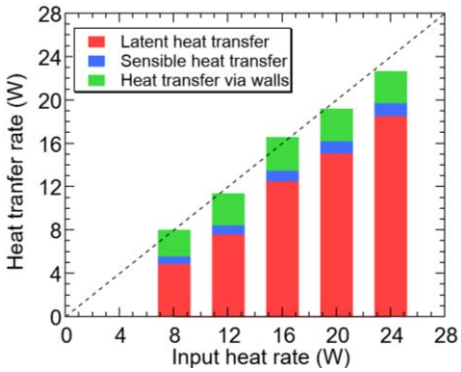

Fig. 2 Experimental input heat rates and heat transfer rates obtained from numerical analysis

Modeling and Fabrication of Thermally-Actuated Bimetal Device

Seungchul OH, Takuma MORI, Kenichi MORIMOTO, Yuji SUZUKI
Department of Mechanical Engineering, School of Engineering, The University of Tokyo
soh@mesl.t.u-tokyo.ac.jp

Bimetal is a device with two metals with different thermal expansion coefficient are attached that converts the thermal energy into mechanical energy directly. For its simple structure, it is a good candidate for micro-scaled heat engine compared to heat engines uses liquid-vapor phase change.

We propose bimetal heat engine by using periodic snap-through vibration phenomenon (Fig. 1a). The device is initially buckled and contacted on the hot source using temperature gradient of the hot source and ambient air. The device releases its stored mechanical energy at once at each snap/snapback moment that delivers large force and deflection.

To design a beam, thermal conduction through support ends and contact force and thermal resistance in the center of the beam should be considered as parameters in order to achieve high frequency and large amplitude vibration at small temperature gradient. We establish an experimental setup that can control each parameter and observe their impacts on frequency and amplitude to optimize the design values of the device. It shows that frequency peaks at certain contact force.

In order to achieve higher working frequency, MEMS technology is used to fabricate the prototype of the device (Fig. 1b). Initial buckled down structure was achieved by controlling the residual stress of the sputtered bimetal film. The prototype device shows snap under 300 ºC and snapback over -78.5 ºC.

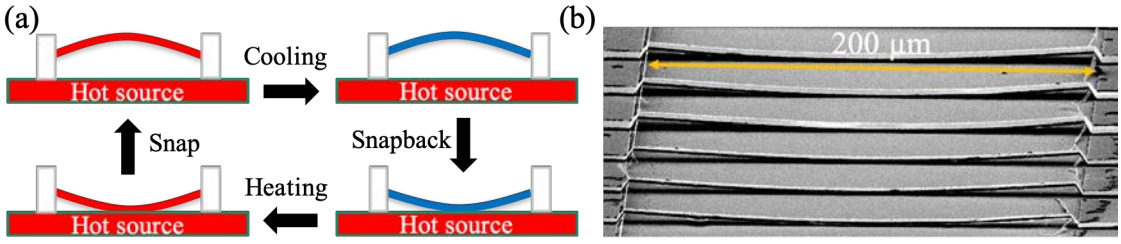

Figure. 1 (a) Concept of bimetal heat engine, (b) The fabricated beam array. Upper/lower three beams have 10 μm/5 μm width each. Initial deflection is 4.5 μm.

Measurement of optical absorption in periodically poled MgO-doped SLT crystals with 532 nm CW laser

Hiroki Emura[1] and Norikatsu Mio[2]

Department of Physics, University of Tokyo[1]

Institute for Photon Science and Technology, University of Tokyo[2]

emura@g-munu.t.u-tokyo.ac.jp

Periodically poled MgO-doped stoichiometric lithium tantalate (PPMg:SLT) crystal is the most promising for a high power green SHG source because of its comparatively high nonlinear coefficient and high thermal conductivity. Yet there has not been a detailed research about its optical absorption and its optical breakdown process. The evaluation of optical properties of PPMg:SLT is necessary to obtain high power green SHG.

In this study, we measured the linear and nonlinear absorption coefficients of PPMg:SLT crystals at 532 nm wavelength by sum of slopes procedure[1] which is one of the calorimetry measurements. Moreover, we investigated the behavior of the optical breakdown. Although the measured absorption coefficients differ among respective samples and respective incident positions, the measurement results suggest that the absorption of the beam polarized along c-axis is larger than that polarized orthogonal to c-axis. In addition, we discuss the phenomena obserbed in the optical breakdown of PPMg:SLT.

[1] Philipp H. Klein, Opt. Eng. **20**, 790-794 (1981)

Analysis of non-equilibrium rarefied gas flows using low variance deviational simulation Monte Carlo

Hiroki Imai

Department of Mechanical Engineering, The University of Tokyo

imai@fel.t.u-tokyo.ac.jp

Evaporation from porous surfaces is ubiquitous in nature, and has also found industrial applications such as desalination systems and micro-pumps. Specifically, high-heat-flux cooling devices have been demanded due to the increasing power densities of semiconductor devices. Nanoporous membrane-based evaporative cooling devices, which can dissipate a heat flux of around 1 kW/cm^2 [1], have recently attracted considerable attentions. The optimized design of these devices requires the understanding of non-equilibrium flow regions near vapor–liquid interfaces; namely, Knudsen layers. Although 1D Knudsen layers have been extensively studied [2], 2D and 3D Knudsen layers have yet to be fully understood. Here, we numerically analyze 2D Knudsen layers to better understand the flow characteristics. Figure 1(a) shows a representative simulation system of the 2D Knudsen layer, and Fig. 1(b) compares the flow fields obtained from direct simulation Monte Carlo (DSMC) and low variance deviational simulation Monte Carlo (LVDSMC). The computational time of LVDSMC is two orders of magnitude smaller than that of DSMC. Additionally, Fig. 1(c) indicates that the number density at the far field asymptotically approaches the counterpart from the 1D Knudsen layer analysis for the smaller Knudsen numbers, while it approaches the result obtained from the macroscopic model for the larger ones.

[1] L. Zhengmao et al., *IEEE Trans. Compon. Packag. Manuf. Technol*. **6**, 1056–1065 (2016).
[2] A. Frezzotti, *Eur. J. Mech B.* **26**, 93–104 (2007).

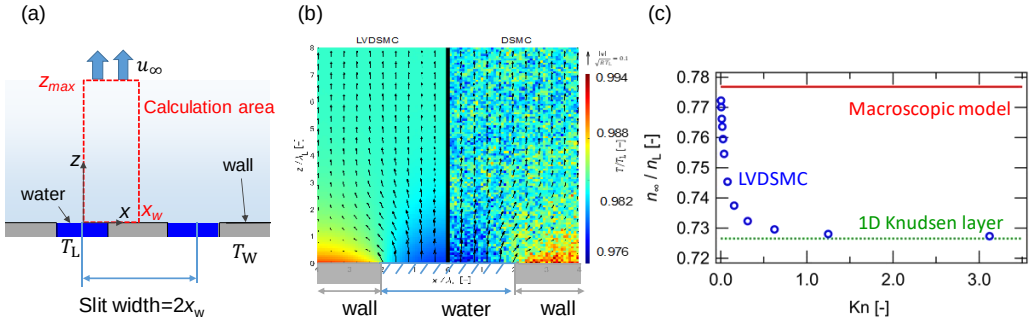

Fig. 1 (a) The simulation system of a 2D Knudsen layer, (b) the flow fields obtained from DSMC and LVDSMC simulations, and (c) the Knudsen number dependence of the number densities at the far field.

Development of ultrafast imaging system using the slicing mirror for understanding the mechanism of laser machining

Takao Saiki[1], Xinyi Qi[2], Ayumu Ishijima[3], Ichiro Sakuma[1, 4, 5] and Keiichi Nakagawa[1, 3, 4]
[1]Department of Precision Engineering, University of Tokyo
[2]Department of Physics and Astronomy, University of California, Los Angeles
[3]PRESTO, Japan Science and Technology Agency
[4]Department of Bioengineering, University of Tokyo
[5]Medical Device Development and Regulation Research Center, University of Tokyo
saiki@bmpe.t.u-tokyo.ac.jp

Laser machining is widely used in the fields of manufacturing and medical industry [1]. Although the detailed mechanism of laser processing has not been elucidated, the processing performance of laser machining depends on technicians' experience and skills. To understand the mechanism and optimize the laser processing, the observation of the plasma evolution is strongly required. Sequentially timed all-optical mapping photography (STAMP) [2] is one method to capture the plasma dynamics. However, the parameters of the imaging performance, such as image quality and number of frames, are limited due to the configuration of the spatial mapping device.

In this study, we developed the STAMP system using a special optics, called slicing mirror, which has tilted 18 mirror facets to produce 18 frames in ultrafast image acquisition of plasma dynamics. As Fig.1 shows, the plasma evolution was observed in 8 frames with a frame interval of 7.9 ps. The results indicate that the system prevents image quality degradation due to an increased number of frames and has potential to acquire information for understanding the details of laser machining.

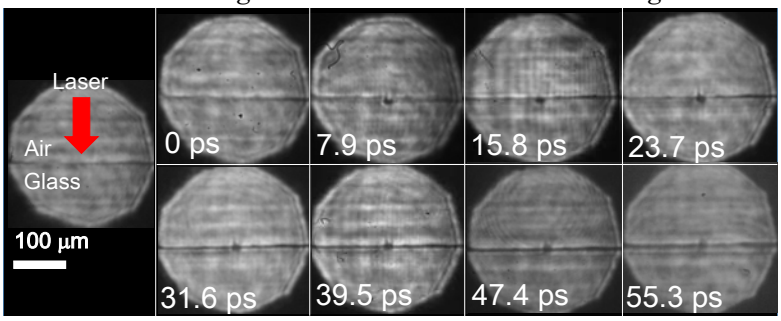

Fig.1: Single-shot imaging of plasma evolution with the frame interval of 7.9 ps

[1] C. Liang *et al.*, Femtosecond Laser Induced Micropattern and Ca/P Deposition on Ti Implant Surface and Its Acceleration on Early Osseointegration, ACS Applied Materials & Interfaces 5, 8179, 8186 (2013).
[2] K. Nakagawa *et al.*, Sequentially timed all-optical mapping photography (STAMP), Nat. Photonics 8, 695–700 (2014).

Electrical property change of woody carbon material by moisture absorption

Nana TAKAHASHI[1], Hiroyuki KUWAE[1], Shuichi SHOJI[1], Jun MIZUNO[2]

1) Electronic and Physical Systems, Waseda University,

2) Research Organization for Nano and Life Innovation, Waseda University,

Email: takahashi@shoji.comm.waseda.ac.jp

We studied electrical property change of natural woody carbon material by moisture absorption. A film of woody carbon material (FWCM), which is a self-standing activated carbon film, was used as a moisture absorbing material. The relationship between resistance and adsorption property of FWCM was evaluated by changing relative humidity (RH) using saturated salt solutions and a desiccant. The mass of FWCM linearly increased by 8.28 μg/mm^2 with increasing according to the chamber RH ranging from 1.5% to 98%. On the other hand, the resistance of FWCM decreased linearly until 75% RH, then it saturated in the high RH condition. These results indicated that the absorbed moisture improved electrical conductivity of the FWCM by transferring charge from adsorbed water molecules to the FWCM surface[1]. This study demonstrates FWCM is expected to have high potentials for a humidity detective material.

[1] A. W. Harding, et. al., Diffusion barriers in the kinetics of water vapor adsorption/desorption on activated carbons, Langmuir, Vol. 14, pp. 3858-3864, 1998.

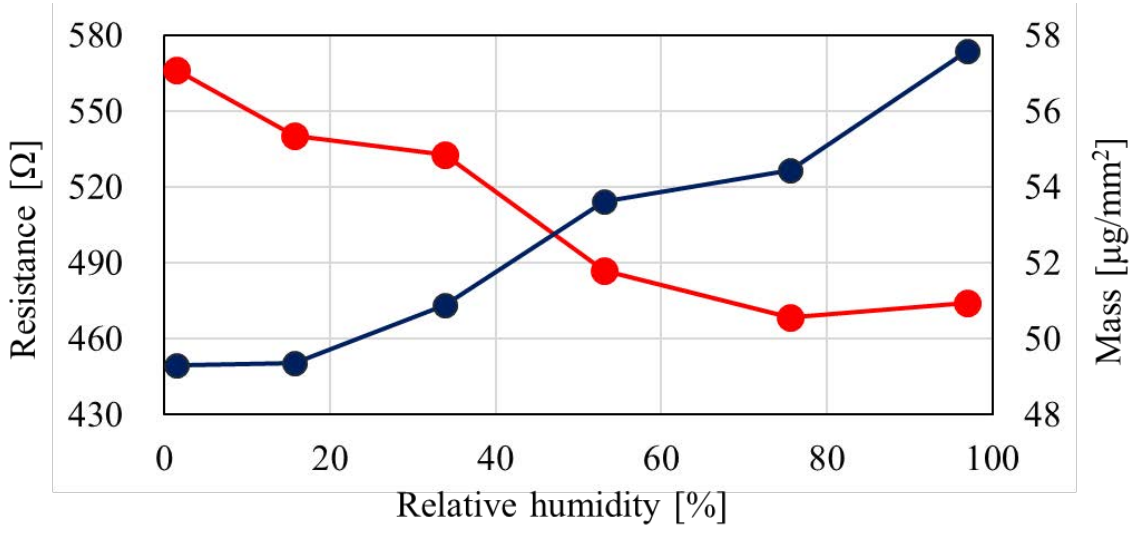

Fig.1 Resistance and mass changes of the FWCM against RH.

Ozone mixed gas grating for high power laser applications

Yurina Michine
Institute for Laser Science, University of Electro-Communications
y_michine@ils.uec.ac.jp

Recently required power and energy of laser systems are increased drastically. The maximum energy of nanosecond laser exceeded Mega(10^6) J and maximum power reached to Exa-watt (10^{18}) level. Even though such inflation of output laser performance, laser induced damage threshold of optics is still remained with several J/cm^2 levels. Therefore, high power laser system size increased year by year. However, some optics (for example, grating) are considered to be beyond present human technology limit. It is strong motivation to develop higher damage threshold optics. For this purpose, we propose ozone assisted gas grating for such high energy laser systems with ultra-high damage threshold. In this method, density modulation is induced with UV absorbed ozone gas molecules. Up to now, we archived (1) high damage threshold for ns lasers (1.6kJ/cm^2) (2) high average diffraction efficiency (<96%) (3) low production energy (<70mJ/cm^2).

Furthermore, applying this ozone gas grating generation method, we propose a new laser focusing system for laser processing and laser plasma generation. This method will reduce the effects of debris, which is an enemy for optics.

High Quality-factor Kerr-lens mode-locked Tm:Sc_2O_3 laser with SRS-based spectral broadening

Anna Suzuki, Masaki Tokurakawa[1], Christian Kränkel[2]

[1]Institute for Laser Science, University of electro-communications

[2]Zentrum für Lasermaterialien, Leibniz-Institut für Kristallzüchtung

a_suzuki@ils.uec.ac.jp

Tm doped materials are very attractive for highly efficient short pulse lasers in the wavelength range of 2 μm due to their broad gain bandwidth and the two for one pumping scheme with 800 nm high power laser diode(LD). Among them, Tm doped sesquioxide (RE=Sc, Lu or Y) are the most promising gain materials as they possess excellent thermos-mechanical properties and a broad gain bandwidth above 1980 nm where less water vapor absorption and Tm^{3+} reabsorption exist[1].

Pulses as short as 115 fs with an average output power of 420 mW have obtained from our Kerr-lens mode locked Tm:Sc_2O_3 laser with a prism pair for dispersion compensation[2]. Here we report on our recent effort towards further pulse shortening by a high quality factor cavity with a chirped mirror instead of the prism pair.

In our experiments, we used a Z-shaped high quality-factor cavity consisting of a chirped mirror of -1000fs^2 (HR>99.9% from 2000 nm to 2200nm) as an end mirror, two folding mirrors (Radius of curvature of 100 mm, HR>99.9% from 2000 nm to 2300 nm) and a OC mirror (transmission of 1%, 0.5% or 0.3% used). The gain medium was Tm^{3+}(1%):Sc_2O_3 with a length of 3.7 mm and a diameter of 7 mm mounted in a water cooled copper holder and placed between the folding mirrors at Brewster's angle. The pump source was a home-built 1611 nm Er:Yb fiber MOPA.

Stable mode-locked operations were obtained with all OC mirrors (Table.1). A maximum average output power of 220 mW with a pulse duration of 80 fs was obtained using 1% OC and the shortest pulse duration of 72 fs with an average output power of 130 mW was achieved using 0.5% OC. Furthermore, using a 0.3% OC, unusual spectral broadening was observed in the 2250-2350 nm region where outside of the gain band of Tm:Sc_2O_3. Calculated from whole spectrum, a transform limited pulse duration seemed to be ~38 fs. This phenomenon would be caused by soliton self-frequency shift [3] sustained by the Raman gain and broad reflection bandwidth of the cavity mirrors. In our current set-up, the cavity has large positive GDD above 2280 nm, so these spectral components could not contribute to pulse shortening. By optimizing cavity GDD design for whole spectral region, much shorter pulse generation would be available.

Table.1 Output properties of ML pulses

OC	P_{ave} (mW)	Δt (fs)	$\Delta \lambda$ (nm)
1%	220	80	65
0.5%	150	72	67
0.3%	50	-	~220

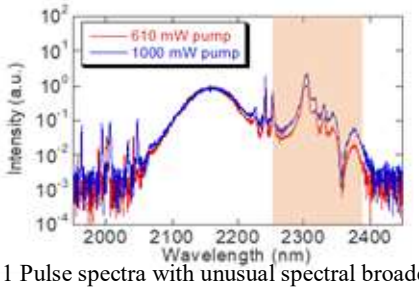

Fig.1 Pulse spectra with unusual spectral broadening

[1] C. Kränkel, IEEE J. Sel. Top. Quantum Electron. 21, 1602013 (2015).
[2] M. Tokurakawa et. al. Opt. Lett. 42 3185-3188 (2017).
[3] F. M. Mitschke et.al. Opt. Lett. 11, 659(1986).

Light Interference Assisted Widening the Wavelength Range of Gold Nanoparticles Coloring and Its Dynamic Control

Bokusui Nakayama [a],*, Keiko Esashika [a] , Yuki Hiruta [a], and Toshiharu Saiki [a]

[a] Faculty of Science and Technology, Keio University, Japan

neomero@keio.jp

The printing technology using ink has problems of color-fading and un-re-writability, and liquid crystal display has problems with the point of power consumption and viewing angle. On the other hand, as seen in stained glass in cathedrals and peacocks' feathers, some of the existing historical artifacts and natural livings exhibit rich colors. Its principles include plasmon resonance and light interference effects, and recent years, by applying these principles, coloring technologies that don't need ink or liquid crystal have been actively developed.

In order to color tuning at the video frame rate, dynamic modulation systems combining Localized Surface Plasmon Resonance (LSPR) and responsive polymer gels have been proposed. By polymerizing, it forms hydrogel, which has drastic volume responsibility to an external field. Much effort has been made to modulate the minute gaps in metal nanostructures by utilizing responsive polymers. However, the color modulation ranges reported by previous researches are all narrow, which are far from practical use.

To solve these problems, we proposed a new technique to widen the wavelength range of coloring by combining the scattering color of gold nanoparticles and the interference color coursed from the gap between the glass and the particles. We prepared a sample including gold nanoparticles (ϕ = 80 nm) well-dispersed in responsive polymer Ploy(N-isopropylacrylamide) (PNIPAM) hydrogel sandwiched by two glass substrates. Light interference occurred for each particle, and when this was combined with the scattering color from the particles, colorful coloring was observed (Fig. 1). In addition, the gel undergoes volume phase transition due to temperature change (Fig. 2). The distance between the substrate and the gold nanoparticles can be controlled and involves the gap length to change. As a result, it was observed the color been tuned according to the temperature change (Fig. 3). We also did theorical calculations, and that showed by changing the material, shape, and size of the particles, the exhibiting color range shifts, that will widen the covering area of the color space.

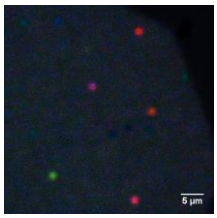

Fig. 1 An experimental image

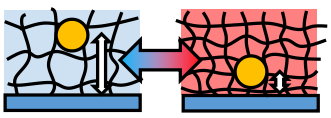

Fig. 2 Schematic of the volume phase transition of PNIPAM gel.

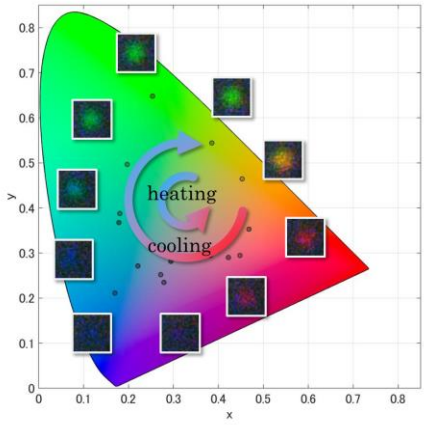

Fig. 3 The transition in color space by changing temperature.

Tunable Dynamics of Janus Particles by Coating Phase-change Material

Ryo Soma[1], Eiji Yamamoto[1], Masashi Kuwahara[2], and Toshiharu Saiki[1]

[1]Graduate School of Science and Technology, Keio University

[2]National Institute of Advanced Industrial Science and Technology

ryo.soma@saiki.elec.keio.ac.jp

Improvement of nano- to microsized fabrication techniques enables various colloidal systems. Designing the diffusive behavior, self-propulsion or self-assembly of colloidal particles has possibility for new devices and modelling active dynamics in nature. Especially, Non-equilibrium transport phenomena of particle with micrometer dimension are associated with a variety of research field. Janus Particles (JPs) are one of the active colloidal particles which are formed with two hemispheres of different substances. Because of their asymmetric properties, JPs generates active swimming motion.

Here we present a study of silica JPs partially coated with a phase-change switching material, $Ge_2Sb_2Te_5$ (GST). In the experiment, alternating electric field was applied. JPs were solvated in distilled water sandwiched by two indium tin oxide coated coverslips as shown in Fig. 1A. Our JPs change their swimming behavior not only by varying alternating electric field but also by switching the phase of GST. At 200 kHz, JPs swim their GST sides facing forward. When GST is amorphous phase (a-GST), they attract each other. However, when GST is crystalline phase (c-GST), JPs repel each other and keep a distance without collision (see Fig. 1B). The transition of dynamics that did not appear in previous metal-silica Janus system can be realized by introducing phase change of GST.

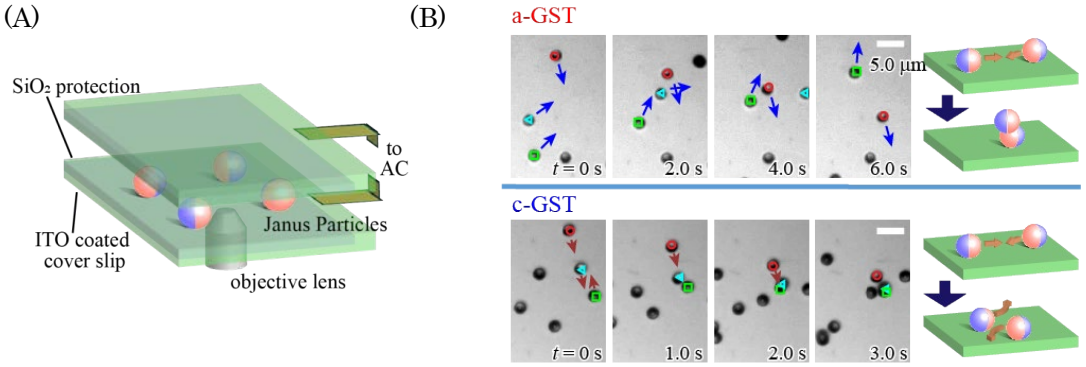

Fig. 1 (A) Schematic illustration of the experiment. (B) The snapshots and schematic illustrations of propelling JPs. V = 6.0 and f = 200 kHz in both cases.

Optical observation of DNA translocation dynamics in SiN nanopore

Katsuyuki Enomoto, Yuki Ishikawa, Hiromu Ishii, Keiko Esashika, Toshiharu Saiki
Graduate School of Science and Technology, Keio University
katsuyuki.enomoto@saiki.elec.keio.ac.jp

Recently, nanopore-based technologies have shown a great promise for developing single-molecule DNA sequencing. Conventionally, two types of measurement methods are used as the nanopore sequencer. Since the method using ionic current has a demerit that only the measurement inside the nanopore can be performed, optical detection capable of observing near the nanopore is effective to know DNA translocation dynamics. In this presentation, we report measurement of salt dependence of single-molecule DNA translocation through SiN nanopores by using blue laser. For this study, we used 20 nm thickness SiN membrane with about 100 nm diameter, blue laser (λ = 488 nm) as the excitation light and 10 kbp DNA sample stained with YOYO-1.(excitation: λ = 491 nm, fluorescence: λ = 509 nm) By applying a voltage across the SiN membrane, the process of DNA translocation through nanopores is optically observed. As the result of measurement, a difference was observed in the increasing region of the fluorescence intensity waveform, and very long rising time that could not be observed in the previous study was confirmed. This is shown in Figures 1 (a) and (b). In addition, the rising time increased as the salt concentration increased. Also, the rising time decreased as a voltage increased. The increase in the rising time may be attributed to the fact that the counterion bind to negatively charged DNA molecule and change their electrophoretic mobility and conformation. Because of a decrease persistence length and stiffness of DNA as the salt concentration increased, it is speculated that the structure of DNA was changed immediately before translocation through nanopores. Also, we considered that as a voltage increases, the inhomogeneity of the electric field near the nanopore increases, which makes it easier for DNA just before translocation through nanopores to be stretched.

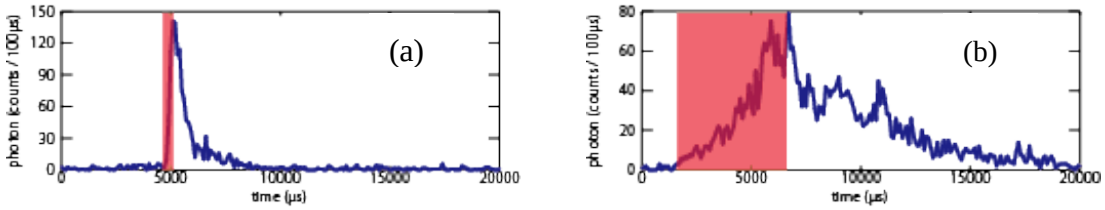

Fig.1 (a), (b) Experimental results of DNA translocation events.

The Development of Flow-type Thermo-electrochemical Conversion Combined with Forced Convection Cooling

Yutaka Ikeda, Yoichi Murakami

Department of Mechanical Engineering, Tokyo Institute of Technology

ikeda.y.ao@m.titech.ac.jp, murakami.y.af@m.titech.ac.jp

Forced-convection cooling is important in wide variety of situations from microprocessors to heat engines. In such situations, active cooling is essential to avoid failures and retain their thermal efficiencies. However, active transfer of large quantity of thermal energy between big temperature difference rapidly destroys the free-energy portion of the thermal energy (*exergy* loss). To address this unresolved problem, we developed the cell as shown in Fig. 1, to simultaneously fulfill the forced-convection cooling of a heat releasing surface and the recovery of the *exergy* loss in the situation of active cooling by incorporating liquid-based thermoelectric conversion (to date has been mainly studied for stationary conditions) into forced-convection cooling[1,2].

In our test cell, the flow was forced to through the inter-electrode channel formed by the cathode (hot side) and anode (cold side). The cathode simulates an object to be cooled by contacting a ceramic heater tightly. We tested three different types of cathodes (#1–#3).

Fig. 2 shows a result of cooling performance, and Fig. 3 shows a electric power generation property (*I*–*V* curve)[1,2]. In this research, we investigated the properties of cooling and power generation, revealed limiting factors on electric power generation through electrochemical analysis and numerical simulations. The details will be presented in this symposium.

[1] Y. Ikeda, K. Fukui, Y. Murakami, *Phys. Chem. Chem. Phys.* **21**, 25838 (2019). DOI: 10.1039/c9cp05028k

[2] Tokyo Tech press release, November 18th 2019, URL: https://www.titech.ac.jp/news/2019/045598.html (In Japanese), https://www.titech.ac.jp/english/news/2019/045723.html (In English).

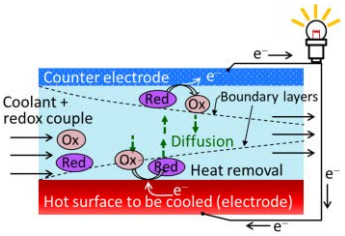

Fig. 1 Schematic illustration of the concept of this study.

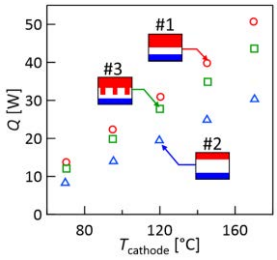

Fig. 2 Dependence of cooling performance on cathode temperature with a flow rate of 0.5 mL/s.

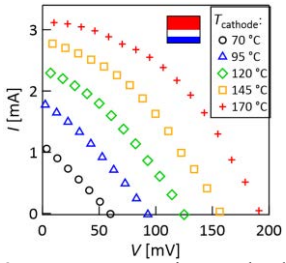

Fig. 3 *I*–*V* curves using cathode #1 with the flow rate of 0.5 mL/s.

Development of laser system of charge exchange process in J-PARC

Aoi Fuchi [1], Yurina Michine, Hiroyuki Harada [2], Saha Pranab, Hitoki Yoneda [1]

[1]Inst. Laser Science, Univ. of Electro-Communications

[2]J-PARC center

a_fuchi@ils.uec.ac.jp

Japanese Proton Accelerator Research Complex(J-PARC) creates MW class proton beam for generation of intense neutron source and meson beam for many applications. This accelerator is consisted of a linear accelerator and two synchrotron accelerators. For efficient transportation and injection of hydrogen ions from the LINAC to the ring-type accelerator, negative H- beam in the LINAC is charge-exchanged and injected into the synchrotron one. Presently, the carbon foil is used for stripping the electrons, but the foil is easily damaged and its life time is only 6 months at the present 300kW operation. In the next JPARC operation plan, a MW class proton beam will be generated so that we need to develop material-free charge exchange method. We propose three-step excitation and ionization process with three lasers. In this paper, we will discuss basic idea of this laser system and efficient using method of the high power laser for the real charge exchange station.

In the laboratory frame, vacuum ultra-violet laser (λ ~ 1000nm) is needed for ionization of hydrogen atoms. To consider high repetition rate(324MHz) of accelerator and more than mJ pulse energy, it is very difficult to prepare such high average power VUV laser with the present laser technology. However, the ion at the linac of the JPARC is already accelerated to relativistic level (400MeV), so Doppler effect which can decrease photon energy will be used by using typical angle of collision between photons and protons. Then, we can determine the wave length using lasers and we have a plan to make three stage charge exchange method as shown in Fig.1. In this scheme, the shortest wavelength laser is 216nm and that wavelength is matched to 5th harmonics of 1064nm laser. Therefore, we can use common oscillator for all three laser pulse.

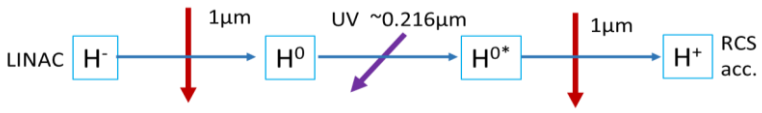

Fig.1 Three stage charge exchange method

Experiments on Polishing Epoxy Resin Surface of CFRP Mirror for Space Telescopes

○Takahito Igawa[*1], Hideo Takino[1], Shin Utsunomiya[2]

[1] Graduate school of Engineering, Chiba Institute of Technology

[2] National Astronomical Observatory of Japan

[*]s1521018vn@s.chibakoudai.jp

To realize carbon fiber reinforced plastic (CFRP) mirrors for space telescopes, high-precision polishing of an epoxy resin surface, which is the reflection surface of such mirrors, is required. To polish the surface with high quality, it is necessary to know the polishing characteristics of epoxy resin. However, unlike acrylic resin, which is a general optical material, there are few studies in which the polishing characteristics of epoxy resin were investigated. Thus, in this study, we polished test pieces of CFRP mirrors and acrylic resin in the same single batch under various conditions, and compared their removal rates. We also evaluated the surface roughnesses for both resins before and after polishing. As a result, we found that polishing conditions using SiC abrasive slurry and a foamed polyurethane pad showed the highest removal rate. In addition, we confirmed that the combination of alumina abrasive slurry and a suede pad provided the required surface roughness.

Appendix

Inside Hongo Campus

① Faculty of Engineering Bldg.1
② Faculty of Engineering Bldg.2
③ Faculty of Engineering Bldg.3
④ Faculty of Engineering Bldg.4
⑤ Faculty of Engineering Bldg.5
⑥ Faculty of Engineering Bldg.6
⑦ Faculty of Engineering Bldg.7
⑧ Faculty of Engineering Bldg.8
⑨ Faculty of Engineering Bldg.9
⑩ Faculty of Engineering Bldg.10
⑪ Faculty of Engineering Bldg.11
⑫ Faculty of Engineering Bldg.12
⑬ Faculty of Engineering Bldg.13
⑭ Faculty of Engineering Bldg.14
⑮ Faculty of Engineering (Reppin-kan)
⑯ Takeda Bldg., Takeda Hall, VLSI Design and Education Center
⑰ Cavitation Tunnel
⑱ Seakeeping Tank; Ship Model Basin
⑲ Seakeeping Tank; Ship Model Basin
⑳ MONOZUKURI Lab.
㉑ Wind Engineering Laboratory
㉒ High Voltage Electron Microscope
㉓ Faculty of Engineering Bldg.12 Annex
㉔ NEW Annex 2
㉕ NEW Tandem Center

Access Map

○ Nearest Station (Walk or bus)

■ Junctions

See campus maps for bus/walking routes from nearest stations.

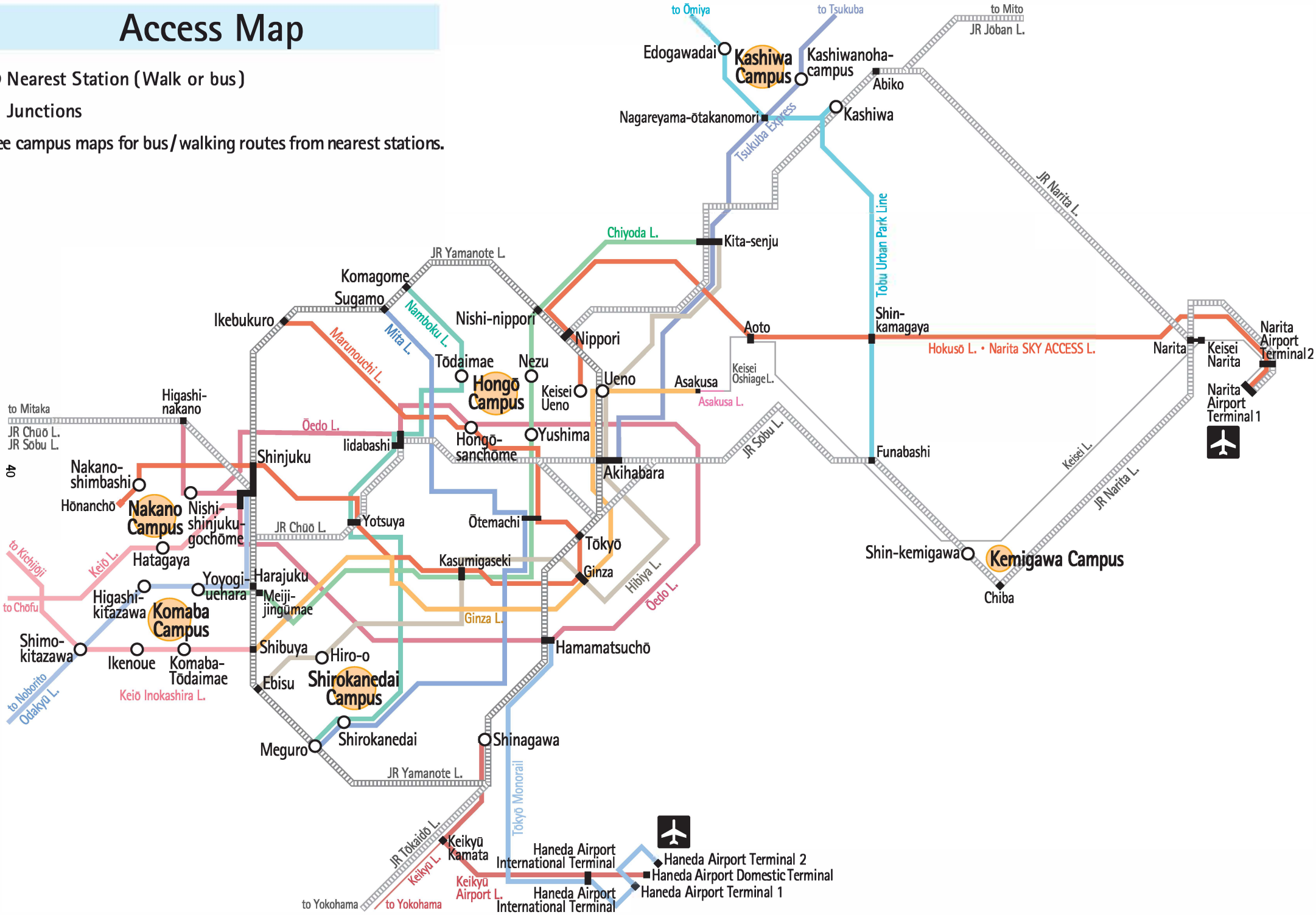

Hongō Campus

Getting to the Hongō Campus

- Hongō-sanchōme Station (Subway Marunouchi Line)
  8 minutes' walk.
- Hongō-sanchōme Station (Subway Ōedo Line)
  6 minutes' walk.
- Yushima Station or Nezu Station (Subway Chiyoda Line)
  8 minutes' walk.
- Tōdaimae Station (Subway Namboku Line)
  1 minute's walk.
- Kasuga Station (Subway Mita Line)
  10 minutes' walk.
- Ochanomizu Station (JR Chūō Line, JR Sōbu Line)
  <Subway>Subway Marunouchi Line (for Ikebukuro)
  → get off at Hongō-sanchōme Station.
  <Subway>Subway Chiyoda Line (for Toride)
  → get off at Yushima Station or Nezu Station.
  <Toei Bus>茶51 for Komagome Station South Exit or 東43 for Arakawa-dote-sōshajō
  → get off at Tōdai-Akamon-mae, Tōdai-Seimon-mae, Tōdai-Nōgakubu-mae stops
  <Toei Bus>学07 for the University of Tokyo
  → get off at Tatsuokamon, Tōdai-Byōin-mae, Tōdai-Kōnai stops.
- Ueno Station (JR Yamanote Line, other lines)
  <Toei Bus>学01 for the University of Tokyo
  → get off at Tatsuokamon, Tōdai-Byōin-mae, Tōdai-Kōnai stops.
- Okachimachi Station (JR Yamanote Line, other lines),
  <Toei Bus>都02 for Ōtsuka Station or 上69 for Otakibashi-shako-mae
  → get off at Yushima-yonchōme, Hongō-sanchōme Eki-mae stops.

1 Yasuda Auditorium	14 Yayoi Auditorium Annex	32 Faculty of Law Bldg.3	53 Ward A
2 Sanjō Conference Hall	15 Information Center	33 Faculty of Law Bldg.4	54 Ward B
3 Ikutokuen (Sanshirō Pond)	16 Sanjō Conference Hall Tatsuokamon Annex	34 General Research Bldg.	55 Central Bldg. (East Wing)
4 Chūō Refectory (Underground)	17 UCR Plaza	35 School of Law Bldg.	56 Central Bldg. (South Wing)
5 Second Refectory	18 Gotenshita Athletic Field	36 Faculty of Letters Bldg.3	57 Central Clinical Service Bldg.1
6 Administration Bureau	19 Baseball ground	37 Akamon General Research Bldg.	58 Central Clinical Service Bldg.2
7 General Library	20 Athletic Field	38 Faculty of Letters Annex	59 First Research Bldg.
8 Shichitokudō (Japanese Sports Gymnasium)	21 Gotenshita Memorial Arena	39 Economics Research Bldg.	60 East Clinical Research Bldg.
9 Administration Bureau Bldg.2	Student Support Center	40 Economics Research Annex (Kojima Hall)	61 Molecular & Life Innovation Bldg.
International Center, Hongō Office・USTEP Office	Disability Services Office	41 Faculty of Education	62 Administration & Research Bldg.
Center for Japanese Language Education	22 Communication Center	42 Faculty of Medicine Bldg.1	63 Clinical Research Bldg.A
Center for Research and Development of Higher Education	23 Overhead Bridge	Harassment Counseling Center	64 South Clinical Research Bldg.
Graduate School of Public Policy	24 Tennis Courts (Under Construction)	43 Faculty of Medicine Bldg.2	65 Clinical Research Ward
Hongō Health Service Center	25 Tennis Courts	44 Medical Library	66 Advanced Clinical Research Center
Integrated Research System for Sustainability Science (IR3S)	26 Tennis Courts	International Research Center for Medical Education	67 Energy Station
10 Kaitokukan	27 Entrepreneur Plaza	45 Faculty of Medicine Bldg.3	68 Faculty of Pharmaceutical Sciences
11 Ikutokudō (Japanese Archery Range)	28 Mukougaoka Faculty House	46 Faculty of Medicine Annex of Bldg.3	69 Pharmaceutical Sciences Research Bldg.
12 Student Counseling Center	29 Itō International Research Center	47 Bioscience Research Bldg.	70 Pharmaceutical Sciences Library
Nandemo-Sōdan (One-Stop Resources) Office	Itō Hall	48 Faculty of Medicine Bldg.4	71 Frontier Sciences for Drug Discovery Bldg.
Communication Support Room	Executive Management Program Office	49 Faculty of Medicine Bldg.5	72 Head Administration Office of Engineering (Reppinkan)
Peer Support Room	Policy Alternatives Research Institute	50 Faculty of Medicine Experimental Research Bldg.	73 Faculty of Engineering Bldg.1
Career Support Office	30 Faculty of Law & Letters Bldg.1	51 Faculty of Medicine International Research Center	74 Faculty of Engineering Bldg.2
13 Yayoi Auditorium	31 Faculty of Law & Letters Bldg.2	52 Clinic	75 Faculty of Engineering Bldg.3

76 Faculty of Engineering Bldg.4	96 I-REF Bldg.	117 Biotechnology Research Center	
77 Faculty of Engineering Bldg.5	97 Faculty of Science Bldg.1 (East) (Under Construction)	118 Food Science Bldg.	
78 Faculty of Engineering Bldg.6	98 Faculty of Science Bldg.1 (Center) Koshiba Hall	119 Life Sciences Research Bldg.B	
79 Faculty of Engineering Bldg.7	99 Faculty of Science Bldg.1 (West)	120 Protein Research Laboratory	
80 Faculty of Engineering Bldg.8	International Center for Elementary Particle Physics	121 Interfaculty Initiative in Information Studies & Graduate School of Interdisciplinary Information Studies	
81 Faculty of Engineering Bldg.9	100 Faculty of Science Bldg.2	122 iii-Fukutake Hall	
Institute of Engineering Innovation	101 Faculty of Science Bldg.3	123 iii-Daiwa Ubiquitous Computing Research Bldg.	
82 Faculty of Engineering Bldg.10	102 Faculty of Science Bldg.4	124 Earthquake Research Institute Bldg.1	
83 Faculty of Engineering Bldg.11	103 Faculty of Science Bldg.7	125 Earthquake Research Institute Bldg.2	
84 Faculty of Engineering Bldg.12	104 Faculty of Science Chemistry Bldg.	126 Earthquake Research Institute Bldg.3	
85 Faculty of Engineering Bldg.12 Annex	105 Faculty of Agriculture Bldg.1	127 Institute of Molecular and Cellular Biosciences	
86 Faculty of Engineering Bldg.13	106 Faculty of Agriculture Bldg.2	128 Institute for Advanced Studies on Asia	
87 Faculty of Engineering Bldg.14	107 Faculty of Agriculture Bldg.2. Annex	129 Institute of Social Science	
88 Takeda Bldg.	108 Faculty of Agriculture Bldg.3	130 Historiographical Institute	
Takeda Hall	Asian Natural Environmental Science Center	131 University Museum	
VLSI Design and Education Center	109 Faculty of Agriculture Bldg.5	132 Micro Analysis Laboratory, Tandem Accelerator (MALT)	
89 Seakeeping Tank; Ship Model Basin	110 Faculty of Agriculture Bldg.6	133 Environmental Science Center	
90 Experimental Tank	111 Faculty of Agriculture Bldg.7A	134 Environmental Science Center Annex	
91 Cavitation Tunnel	112 Faculty of Agriculture Bldg.7B	135 Isotope Science Center	
92 Monozukuri Lab.	113 University Library for Agricultural and Life Sciences	136 Information Technology Center	
93 Power Dynamics Experiment Laboratory	114 Agricultural and Life Sciences Museum	137 Information Technology Center Annex	
94 Wind Engineering Lab.	115 Life Sciences Research Bldg.	138 Cryogenic Research Center	
95 High Voltage Electron Microscope	116 Veterinary Medical Center		2016.5

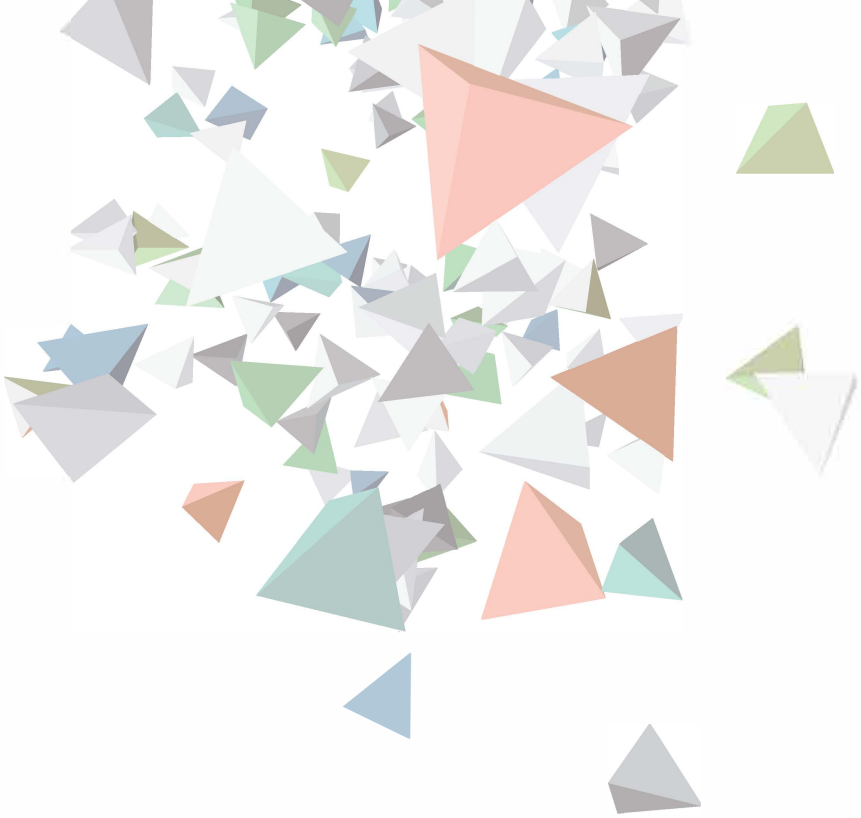

CIAiS

Research and Education Consortium for Innovation of Advanced Integrated Science

GMSI Office, The University of Tokyo
ENG.Bldg.2-203 7-3-1 Hongo, Bunkyo-Ku, Tokyo, 113-8656, Japan
TEL&FAX:03-5841-0696 Email:office@gmsi.t.u-tokyo.ac.jp
http://ciais.t.u-tokyo.ac.jp/